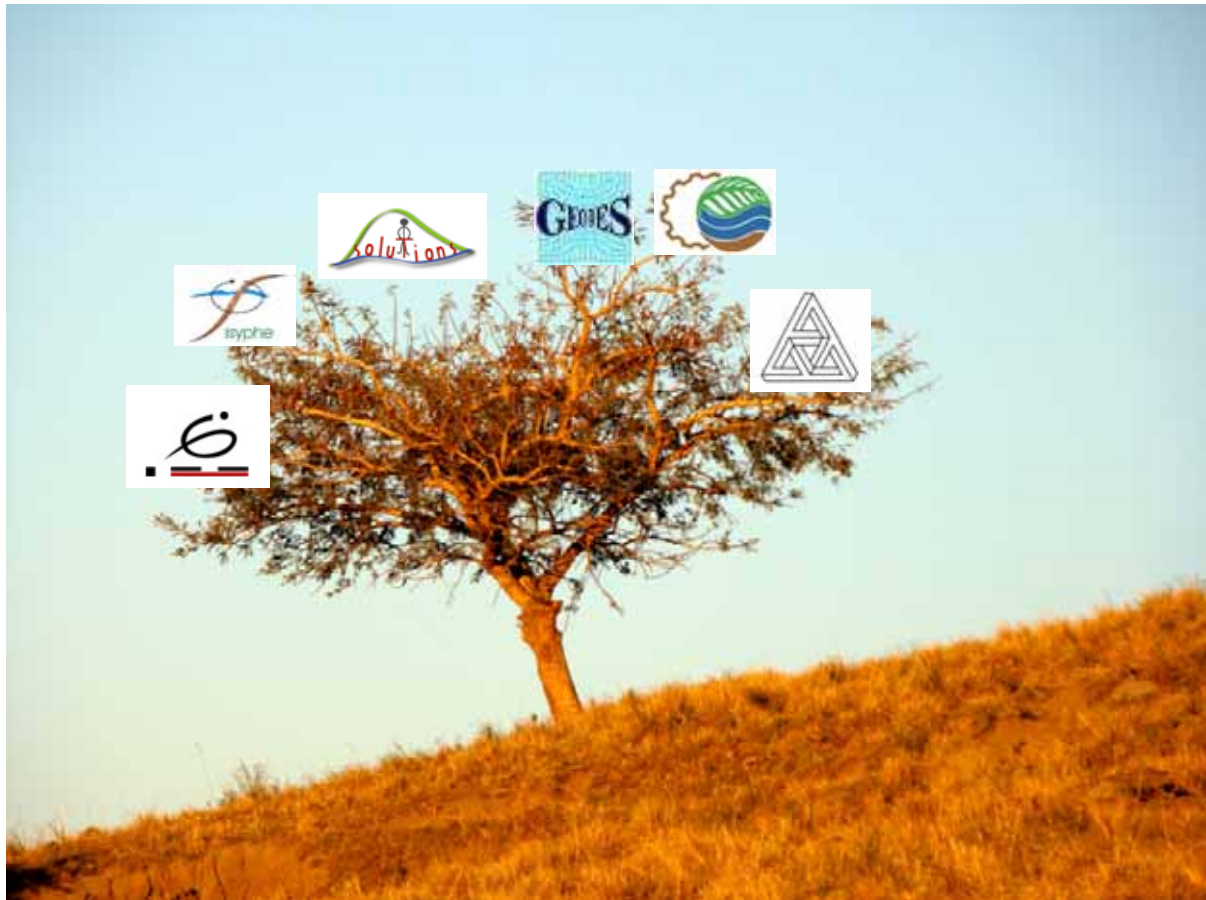


# POTSHINI

Geophysical report of the June and July campaigns  
2008



**Nicolas Florsch** (*coordinator*)

**Christian Camerlynck**  
**S raphine Grellier**  
**Jean-Louis Janeau**  
**Henri Laurie**  
**Simon Lorentz**  
**John Kalela Ngeleka**  
**Myriam Schmutz**

*November 2008*

## **TABLE**

Introduction	3
Surveys using EM31 and EM38)	5
EM31	6
EM38	11
Vertical electrical soundings	33
Electrical resistivity tomography	39
Time domain electromagnetic	41
Conclusion	43
ANNEXE 1: perspectives	45
ANNEXE 2: water conductivity measurements	46
ANNEXE 3: Terrameter 1000 use, memento	47
ANNEXE 4: Location of the Vertical Electrical Soundings	49



## Introduction and reminds

The geophysical methods used in Potshini are aimed at helping to understand the functioning of the local ecosystem, and especially to find out those of the features of the soil that could play an important role in it. It is used here to contribute to understand the interactions among woody-plant encroachment, subsurface water and gullies at the hillslope scale. In the pastures considered pastures, the specie *Acacia Seiberiana* is an alien, but the question of its exact rule is open: bad or good for sustainability?

During this campaign only electrical and electromagnetic methods have been used<sup>1</sup>. The link between the output of geophysics, that is a 2-D or 3-D description of some physical parameters of the subsurface and ecosystems appears when considering that the methods used here are sensitive to the water and electrolytic content of the ground. All provide electrical resistivity or its inverse, conductivity<sup>2</sup>. Note that this report only mentions preliminary investigations. Further experiments, campaigns and interpretation will complete the work.

We recall first (briefly) some of properties of rocks and they reveal the possible benefit of our geophysical methods on this field.

### Electrical properties of rocks: determination of porosity and permeability

The most classical relationship between the effective conductivity and the water content is Archie's law, valid in the case of water-saturated materials. First let us note:  $\sigma_{\text{eff}} = \frac{\sigma_w}{F}$  where  $\sigma_{\text{eff}}$  is the effective conductivity,  $\sigma_w$  is the conductivity of the impregnation water and F is called (by definition) the "formation factor". Archie's law states that  $\sigma_{\text{eff}} = \frac{\sigma_w}{F} = \sigma_w \Phi^m$ , where  $\Phi$  is the porosity. According to Archie (1942), the exponent m increases with cementation, from m=1.3 for sands to 2 for consolidate sandstones.

However this first law has been established for clay-free materials, and is only relevant to bulk conductivity so its use is limited.

A more common relation takes into account for the "surface conductivity", that is either surface conductivities on grains or on clay plates or both when clays coat the grains). Actually the available ions to permit this conductivity are provided by the double-layer.

The relation is written:  $\sigma_{\text{eff}} = \frac{\sigma_w}{F} + \sigma_s$  (see note<sup>3</sup>), introducing an implicit surface conductivity  $\sigma_s$  (Schön, 1996). It can be linked with the cation exchange capacity, as shown by Waxman and Smits (1968), or can be measured experimentally by fitting the law. The surface conductivity  $\sigma_s$  can be estimated in the lab by measuring the conductivity of samples by varying the impregnation water conductivity. This could be useful in Potshini. The most advanced model for conductivity is probably the one by Pride, 1994 (see BOX 1 further).

---

<sup>1</sup> Other methods will be useful: seismic refraction to delineate the rocky basement and magnetic prospection to map the dolerite intrusions, while Spontaneous Polarization (SP) could provide the water table depth.

<sup>2</sup> Although they are linked by resistivity=1/conductivity, they are not equivalent in practice: inductive methods better see conductive bodies while galvanic methods are (relatively) more sensitive to resistive bodies.

<sup>3</sup> Hence this formation factor is the one "assuming there is no surface conductivity". Numerous authors prefer to keep the original definition of F as the ratio between the resistivity of the rock and the resistivity of the water it contains.

In a non-saturated medium, the basic Archie's law is rewritten:

$$\sigma_{\text{eff}} (\text{saturated}) = \sigma_{\text{eff}} (\text{unsaturated}) \cdot S^d,$$

where (S) is the saturation index and (d) varies between 1.3 and 2, and generally is close to 2 for consolidated rocks.

From that, one would be satisfied if it was possible to retrieve the relevant hydrological parameters like the hydraulic conductivity (K) or the hydraulic permeability (k). It is not yet simple. Many attempts have been made by using a relation of the form:  $k = \frac{1}{aF\Sigma}$ , where  $\Sigma$  is the specific surface area (ratio of the pore surface over pore volume).

One of the most promising methods to retrieve the permeability is based Induced Polarization methods, more exactly determining the relaxation time constant ( $\tau$ ) of the electrical response<sup>4</sup>. This is still a matter of purely methodological research (see Binley *et al.*, 2005).

### *BOX 1: Hydrogeophysical and hydrogeological perspectives*

Actually there is no general fully satisfying model to deal with rock resistivity, water content, and clays.

One of the most commonly used empirical equations to predict the electrical conductivity of soils in terms of water content is that of Rhoades *et al.* (1976). It is directly written (with  $\theta$  the water content):

$$\sigma_{\text{eff}} = \sigma_w \theta T_c(\theta) + \sigma_{\text{surface}}, \text{ where } T_c(\theta) = a\theta + b.$$

The "transmission coefficient"  $T_c(\theta)$  is assumed to be a linear function of  $\theta$ , where a and b are empirical and depend on the soil type. Rhoades *et al.* (1976) provided  $a=2.1$  and  $b=-0.25$  for clay soils, and  $1.3 \leq a \leq 1.4$  and  $-0.11 \leq b \leq -0.06$  for loam soils.

Practically: after having estimated  $\sigma_{\text{surface}}$  (and possibly (a) and (b)) by fitting the law in the lab, geophysical surveys may be transformed into water content information, by using this relationship. This is how the geophysical data can be used here, qualitatively and quantitatively.

A practical form is provided in the recent paper by Giroux and Chouteau, 2008, and particularly formula (3) page 1084 and the appendix A.

These theories can be applied at Potshini, and may serve our main hydrogeophysical aim, that is to interpret two geophysical images surveyed during two distinct hydrological regimes, providing a differential image which reveals the displacement of the water between the two states (and later to link that with ecological patterns).

---

<sup>4</sup> We expect the law  $k \propto \tau/F$ , see for instance Kemna, 2000.

The application of geophysics at Potshini concerns an ecological question, and refers to the encroachment of *Acacia sieberiana*. Correlating geophysical output with a map of the various plants is relevant. Further work will lead to understanding of the water flows in the ground and is expected to improve the understanding of this ecosystem.

During this campaign, we followed a dual strategy: one static (pure mapping) and one was dynamic, requiring the maps to be measured again in the wet season to detect seasonal changes.

Completing the geophysical approach should involve more field investigation tools, mainly a extensive SP survey (at least detailed on the toposequence) to try to determine the water table depth (that is only feasible after a significant period of rain since it is the water flow itself which induces the signal), and a magnetic prospection will be useful to localize the dolerite dykes.

### 1. Surveys using the Slingram EM31 and EM38.

They are inductive methods. One coil serves as a transmitter and produces an alternative magnetic field in the ground (9.8 kHz for the EM31 and 14.6 kHz for the EM38). As a first approximation, we have the following: this magnetic field induces an electric field in the ground as stated by the

Maxwell equation  $\nabla \times \vec{E} = -\frac{\partial \vec{B}}{\partial t}$  ( $\vec{E}$  electric field and  $\vec{B}$  magnetic induction). The induced electric

field leads to a density current  $\vec{J} = \sigma \vec{E}$  where  $\sigma$  is the conductivity (they are often named “eddy currents” due to the rotational pattern). These currents produce a secondary magnetic field which is detected by the receiving coil (in which it is stacked with the primary field caused by the transmitter loop).

Hence the secondary field reflect the conductivity.

The depth of investigation is mainly depending on the coils separation (s), but also depends on the direction of the coils axes. In Geonics devices, the coils are supposed to be at the same height above the ground, and two modes are used: the vertical dipole mode in which the two coil axes are vertical, and the horizontal one.

The depth of investigation can be discussed by considering the detection of a thin conductive horizontal layer at a given depth, saying (h). Let be (s) the coil spacing. Then, in vertical mode, sensitivity is null at the surface, then reaches a maximum at  $h=0.4s$ , and then decays progressively. In the horizontal mode the sensitivity is maximum at the surface and decreases quickly with depth. (See Figure 9 in the EM38 section).

We have  $s=3.66$  m for the EM31 and  $s= 1$ m for the EM38.

*BOX 2: how EM31 and EM38 works on layered media?*

In the case of an horizontally layered subsurface, a superposition principle permits one to calculate an apparent conductivity  $\sigma_a$ . For instance, considering a two-layer system with a superficial layer of conductivity  $\sigma_1$  over bedrock of conductivity  $\sigma_2$  at a depth  $h$ , we get for the vertical dipole mode: (with  $z=h/s$ ,  $s$  being the coil spacing):

$$\sigma_a = \sigma_1 [1 - R_v(z)] + \sigma_2 R_v(z), \text{ with } z = \text{depth}/s \text{ and } R_v(z) = \frac{1}{\sqrt{4z^2 + 1}}.$$

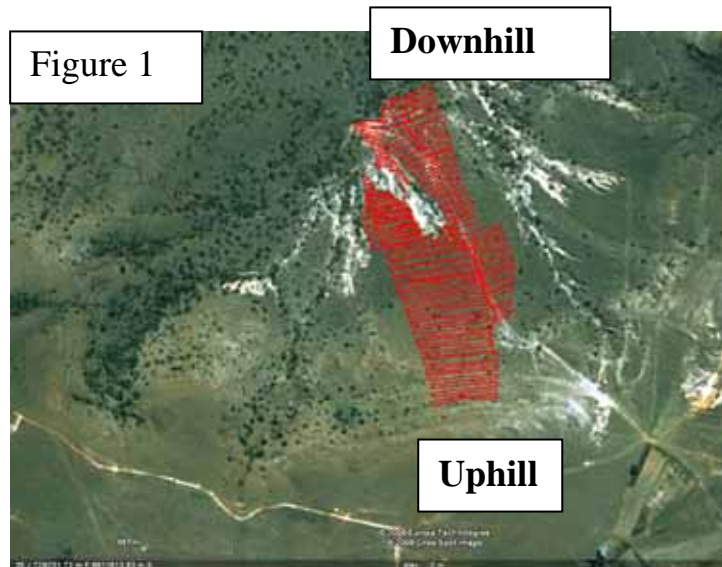
If we combine vertical and horizontal modes of both apparatus EM31 and EM38, we get 4 independent parameters which allow some suitable procedure to derive the shallow stratification. (It requires an inverse algorithm like least-squares, but a Bayesian formalism is probably better to study the parameter covariances).

In the case of 3 layers, we get  $\sigma_a = \sigma_1 [1 - R_v(z_1)] + \sigma_2 [R_v(z_1) - R_v(z_2)] + \sigma_3 R_v(z_2)$ .  
And so on.

A comprehensive and complete manual of how and for what purpose to use Slingram can be found in the technical note TN6 provided by Geonics on its Internet site:

<http://www.geonics.com/html/technicalnotes.html>

### 1.1. EM31 at Potshini



We performed two operations. The first is devoted to a general “static” map<sup>5</sup>. This is done by fixing a walking GPS on the apparatus and then by walking over the whole prospect along profiles spaced out by approximately ten meters. Figure 1 shows the pattern of that coverage on the studied area, while the Figure 2 shows Christian operating the Slingram. Coils are small ones within the ends of the tube.

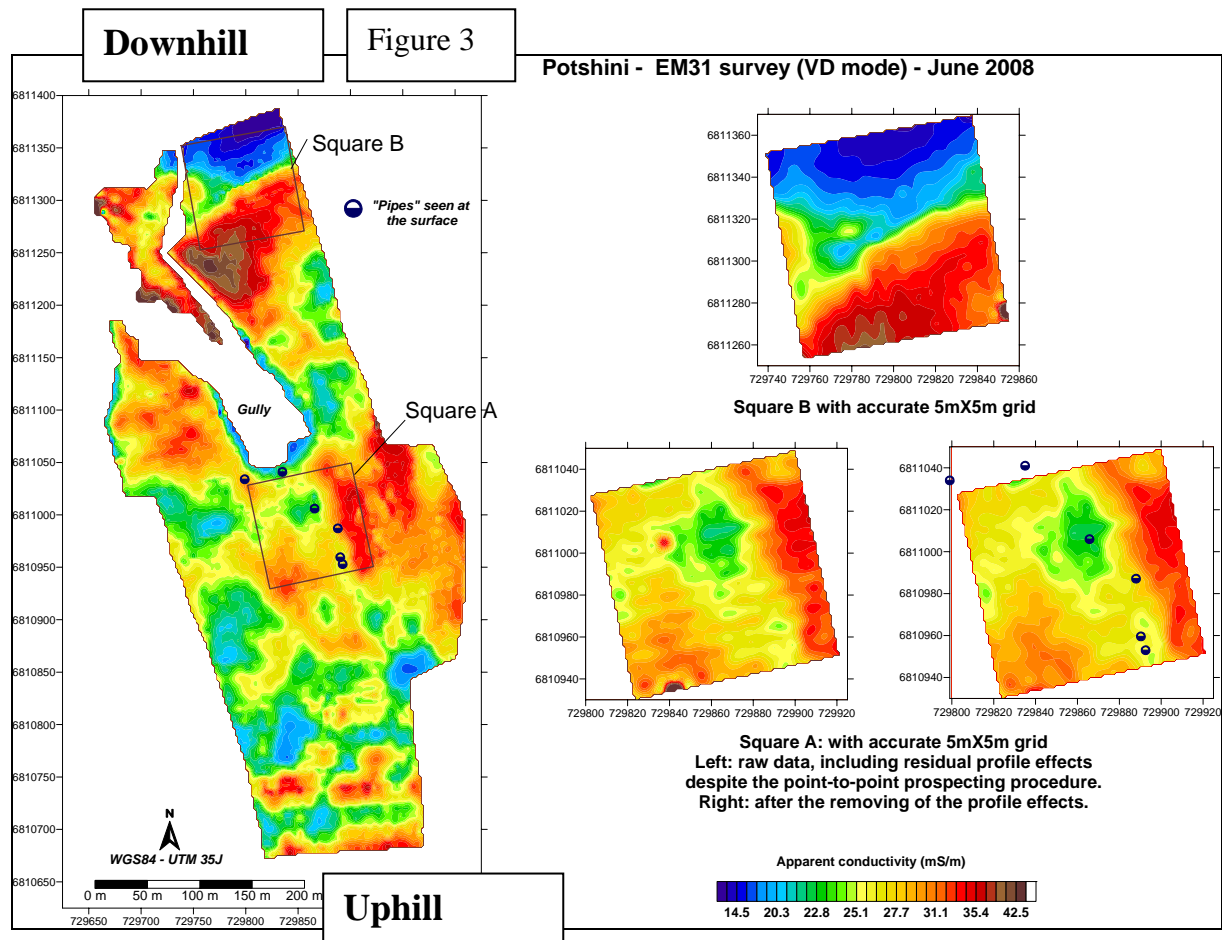


The second operation consisted in detailing two chosen 100mX100m prospects which are depicted on Figure 3. Here the mesh is accurate and the gridding is exactly 5mX5m. It is in these two areas that the accuracy of resistivity changes over time will be the stronger, since it will be possible to redo the measurements at the same locations. Although such a repetition can be performed on the whole area, it will be less quantitative and more qualitative.

<sup>5</sup> In fact it will be useful to redo it during the wet season ; but at this stage we cannot guarantee that the data will be usable for time-lapse study since the survey was made by “walking” on the field with random (but known) trajectories it will be difficult to reproduce.

This two step operation is strategic: measuring the whole prospect by using a 5MX5M grid would have been too much time consuming!

The depth to which the device has its peak of sensitivity is normally close to 1.5 m (TN6 in BOX2). However the instrument is carried above the ground at 1 m height. Then it is generally considered that the apparent conductivity reflects a weighted real conductivity from the surface to about 5 or 6 m depth, with a weighting function progressively decreasing with depth. So the conductivity provided by the EM31 reaches depths where the evapotranspiration at the surface has no influence on the water content (but of course tree or fynbos-like roots may play a role!).



Notice that the difference between the results of the walking-GPS method and those obtained by using the accurate 5mX5m meter-tape method is not important.

Now let us comment this picture, after some zooming on Figure 4.

# Potshini - EM31 survey (VD mode) - June 2008

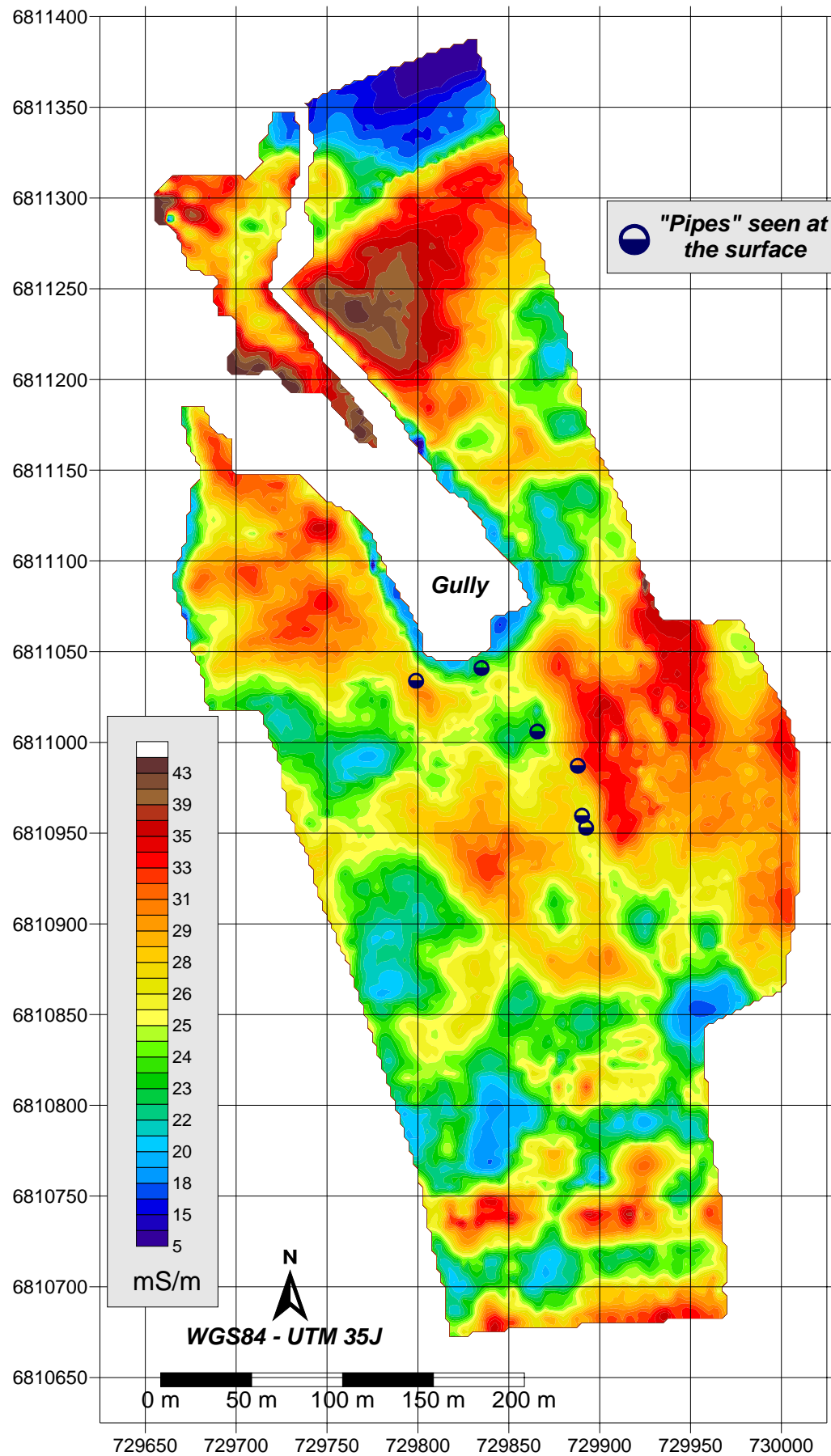


Figure 4

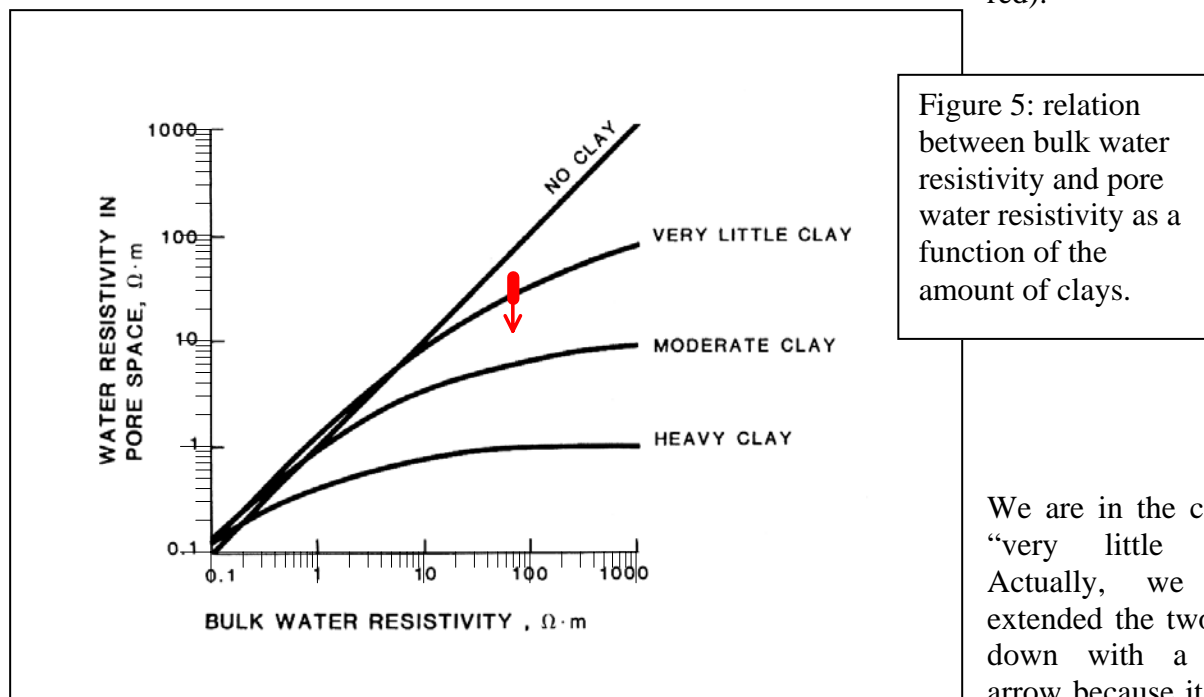
## Comments

The conductivities lie between 10 and 50 Sm/m, most values being between 20 mS/m and 40 mS/m. At the top of the slope some alternations of more or less conductive patterns is consistent with the bedding of more or less consolidated sandstones banks which intercept the surface. One can consider that it fixes here the typical expected conductivities that will be encountered on the whole prospect at mean depth (50 cm to 2 m), and, except for the lower area in the North (and except for some additional but rare deviations elsewhere, it is true).

The water resistivities have been measured at various location on the surface, after percolation (see the table in the annexé), and vary from 14 mS/m to 17 mS/m downstream where the water could be high in carbonic acid. In the well -on the other side of the hill- the conductivity is higher with 24 mS/m, however its waters may have been contaminated by human activity or pump oxidation- we don't include this value in the discussion.

We can take a conductivity of 15 mS/m as realistic to continue. Hence most of the extreme values for the ratio  $\sigma_{\text{water}}/\sigma_{\text{ground}}$  values lie between  $15/50=0.3$  and  $15/10=1.5$ . We do not assume here that the saturation is reached, and hence the formation factors will be lower.

We can put those values – converted in resistivities- on the diagram Figure 5 by Keller 1967 (in red):



We are in the case of “very little clay”. Actually, we have extended the two ends down with a small arrow because it could

be like this if we reach the saturation (that is, the current values slightly underestimate the clay amount).

Hence, the whole map can be interpreted as follow:

- resistive parts (in blue) are the more consolidated rocks with the less amount of water or less amount of clay
- conductive parts (the red pole) probably involve a significant amount of water up to the depth of investigation of the EM31 (saying from the surface to 6 m, although we do not have details but an averaged value), or a higher amount of clay.

There is one way to separate the water amount hypothesis from the clayey amount hypothesis: by taking samples on the field and by characterizing them (in term of resistivity, porosity, permeability...). A very few samples will be enough to light up the full survey! We expect that the measurement off samples conductivities will allow us to transform these geophysical data and map into a hydraulic conductivity map.

At the North part of the map we can see a significant boundary, as if there was a wall stopping the water flow, with conductivities lower than 10 mS/m. This is probably due to a lateral geological change. There is a change in topography in this area, and the increase of resistivity coincides with a descending bank about 50 cm height. However, the underground resistivity clearly changes, so it cannot be a simple topographic effect. Moreover, if it was only topographic, the lower part would possibly have been more wet and hence more conductive: but we observe the opposite.

### **About the pipes:**

No convincing correlation can be found between the pipe occurrence and the conductivity map. It means that the pipes do not cause or are not the effect of features that manifest themselves by geoelectrical changes at the scale of the bulk volume involved by the EM31 individual measurement. But this is only valid during the dry season and must be tested also when the weather is rainy.

### **Other features**

- The strip along the gully is only a border effect (miss of matter close to the top of the gully cliff)
- Globally the conductivity could be found higher at the North and lower part and in the middle area (with are also the less sloping part) than at the south where the slope is higher. It is not surprising because consistent with water accumulation there.

### **EM31 first conclusions**

No conclusion before compilation with the other methods! This set of data must be compared with other geophysical surveys, and in the perspective of the motivating question: are the observed variations correlated with surface states, arrangements of plants and topographic indexes? It will definitely be useful to understand the hydrogeological functioning of the area.

We could expect that the drainage ditch (the donga) would have lowered the superficial aquifer. How and why the gully (donga) has no visible connection with the local shallow hydrology?

A possible interpretation is that the waters in the ground are only retention water, and this hypothesis is consistent with the fact that these measurements are done during the dry season. It would implies that this map reveals the state of the retention water (and the amount of clay) in the system during this kind of period. This will be clearer when a set of data will be acquired on the same area with the same method during the wet season.

Geolocalized field samples will also be useful to interpret this set further.

## 1.2. EM38 at Potshini

### Previous considerations

The procedure and theory is similar to the one performed with the EM31, but:

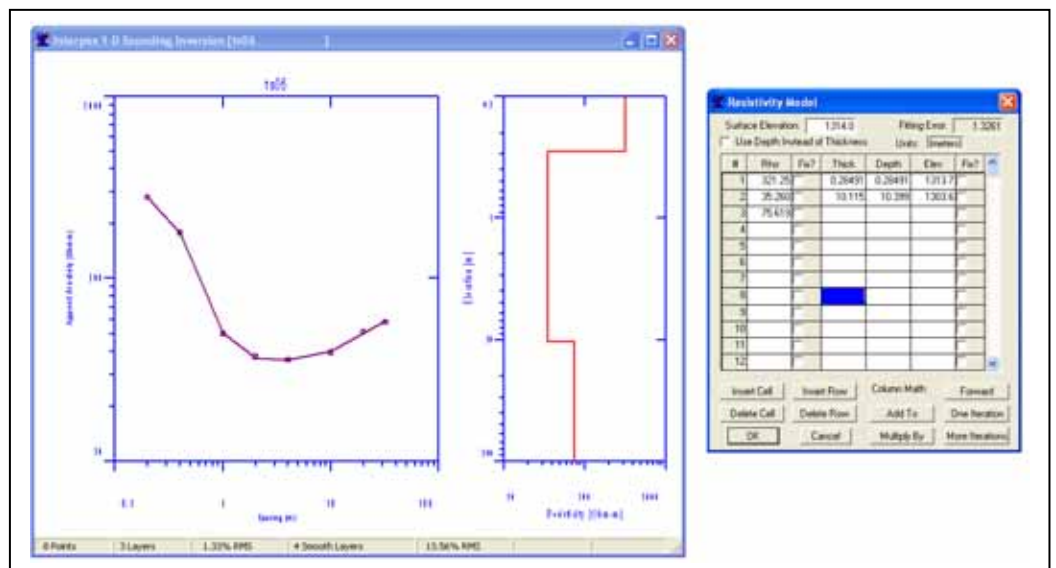
- of course the scale is different, with  $s=1\text{m}$  the EM38 reach a maximum of sensitivity at a depth of 0.4 m (for the vertical mode);
- we surveyed those squared areas already surveyed with a rigorous grid by using the EM31 to be able to follow the time-lapse changes in the conductivity due to changes in water content depending on the season. These squares are located on Figure 3.

The EM38 is undoubtedly the most interesting geophysical method/instrument to be used to contribute (as a geophysical tool) to ecology at Potshini. We shall see that it is also the most tricky and that we did not completely succeed in using it this time. However, we try to deeply analyse “what and how” we can do with it as far as possible improvement are concerned. To do that we shall use Bayesian inversion.

What can we do and expect from EM38? Let us first consider a representative electrical sounding, it is TS06, Figure 7. The first layer is *resistive*: neither clay nor water during this dry season (typically  $300 \Omega \cdot \text{m}$  or more or less  $3 \text{ mS/m}$  in conductivity). A second layer is *conductive* with a  $35 \Omega \cdot \text{m}$  or a conductivity close to  $30 \text{ mS/m}$ . The thickness of the resistive layer is about 0.3 m.

**Figure 7: a typical VES showing the first resistive superficial layer followed by a conductive and clayey layer.**

**VES locations are given in ANNEXE 4**



These features are easily recognizable on the field, see the following Figure 8. The soil horizon O is almost non existing. The horizon A matches the resistive layer, which is poor in clays and water, while the B and C horizons are the found conductive layers.

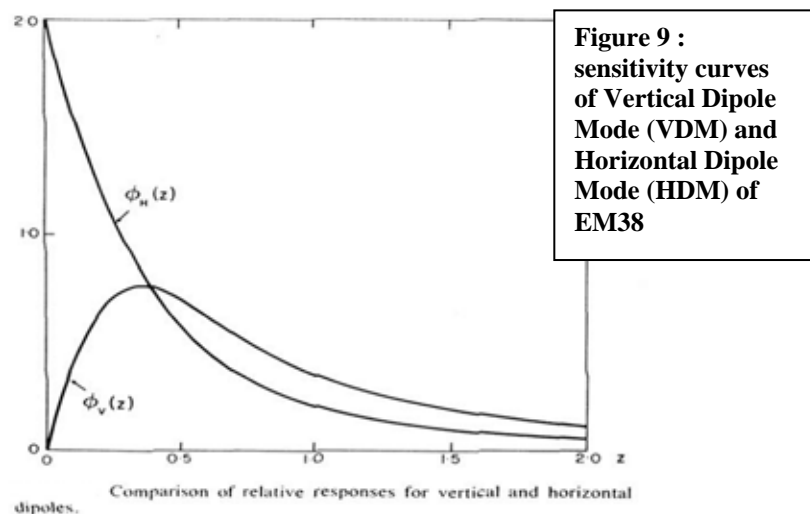
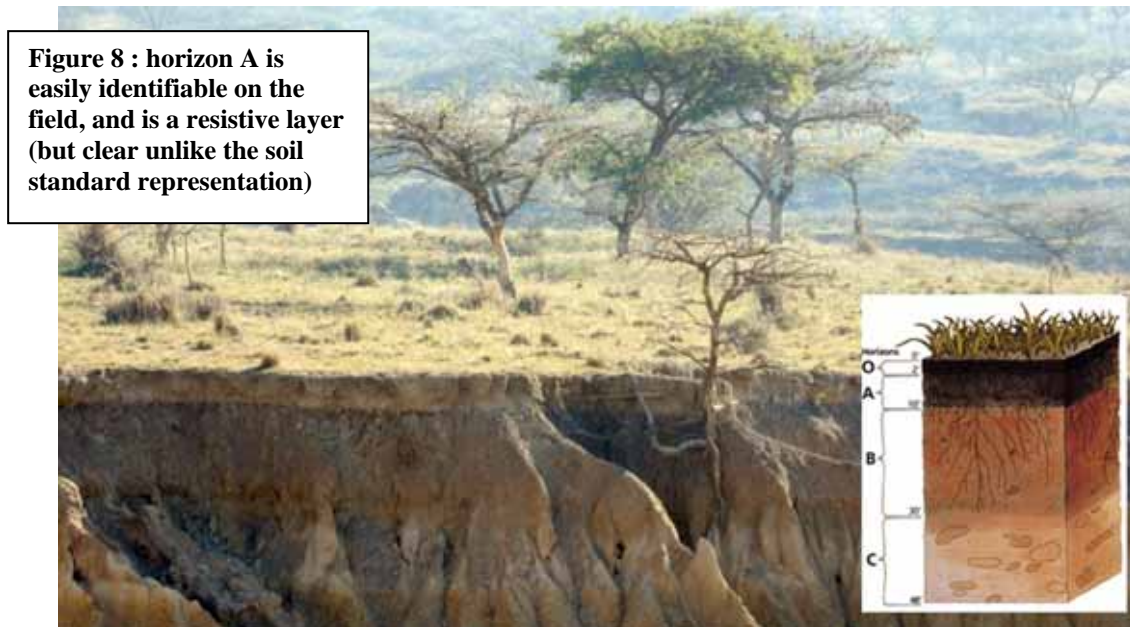
What will the EM38 be sensitive to? In TN6 from GEONICS, this question is addressed by plotting the response of the device to a thin conductive layer. We reproduce it below, Figure 9.

- The VD (Vertical Dipole) mode will not be very sensitive to the first resistive layer, since the maximum of sensitivity is as 0.4 m. However it will be sensitive to the *depth* of the top

of the conductive layer, and also will be sensitive to the second (and conductive) layer conductivity.

- The HD mode is *relatively* more sensitive to the most superficial layers, approximately in the first twenty centimetres. It will also be depending on the depth of the corresponding first interface.

Now notice that the measurements of the VD and the DH mode provides only two parameters, while in our elementary model, three parameters have to be retrieved: ( $\sigma_1$ ) the conductivity of the first layer, ( $\sigma_2$ ) conductivity of the second layer, and (h) the interface depth. So, one idea is to add an additional independent measurement, and we suggested to take a measurement in the DV mode, but handling the device at 50 cm (exactly) above the ground<sup>6</sup>. Other measurement could be used assuming a sensitivity to these depths, like electric measurements, but the advantage of using the same apparatus is clear. By using such a procedure, we get something close to 3 independent combinations of our 3 parameters (see BOX 3).



<sup>6</sup> A 10 cm variations (or even less) in the height of the device would produce a noise preventing good inversion.

*BOX 3: the EM38 with 3 measurements: basic equations*

As seen in BOX 2, the response of the EM38 (case  $s=1$ , and  $z=h/s=h$ ) in the case of the DV mode and a two layer model is (with a superficial layer of conductivity  $\sigma_1$  over bedrock of conductivity  $\sigma_2$  at a depth  $h$ ):

$$\sigma_a^V = \sigma_1 [1 - R_V(h)] + \sigma_2 R_V(h), \text{ and } R_V(h) = \frac{1}{\sqrt{4h^2 + 1}}. \text{ In the HD mode, it is similar:}$$

$$\sigma_a^H = \sigma_1 [1 - R_H(h)] + \sigma_2 R_H(h) \text{ but with } R_H(h) = \sqrt{4h^2 + 1} - 2h \text{ (see TN6 from Geonics).}$$

In the DV mode with the instrument handled 50cm above the ground, one gets an additional air layer (conductivity=0) and the depth is increased by 50cm. Applying the formula to the three layer case with a null first layer conductivity provides:

$$\sigma_a^{V05} = \sigma_1 [R_V(0.5) - R_V(h + 0.5)] + \sigma_2 R_V(h + 0.5).$$

$\{\sigma_a^V, \sigma_a^H, \sigma_a^{V05}\}$  is the set of values to be measured on the field and later inverted to recover  $\{\sigma_1, \sigma_2, h\}$ : it is a non-linear system of 3 equations with three unknowns, and the non-linearity of the whole is a consequence of the non-linearity with respect to  $h$ .

Now we seem to have at our disposal a suitable method to retrieve the horizon A main geoelectrical parameter (assuming a good correspondence between the identity of the layers and the electrical contrasts). But how to really establish the validity of that assertion? Is it enough to get the inverted parameters, for instance by using a least square method? At least valuable error bars must be provided!



In the frame of Potshini investigation, we explored several inverse schemes to retrieve the 3 parameters, and found out that despite the apparent simplicity of the problem, it is not at all a simple issue<sup>7</sup>.

*BOX 4: solution assuming  $\sigma_1 \cong 0$*

We first considered a simplified problem, which could be useful and of interest in the case where  $(\sigma_1)$  is small. That is, let us assume that  $\sigma_1 \cong 0$ . Then only two measurements are required, saying  $\{\sigma_a^V, \sigma_a^H\}$ . This leads to an easy determination. Let set  $\mathfrak{R} = \frac{\sigma_a^H}{\sigma_a^V}$ . After some

elementary calculations, we get:  $h = \frac{1 - \mathfrak{R}}{2\sqrt{2\mathfrak{R} - 1}}$ . Does this exist? This is possible only if

$2\mathfrak{R} - 1 > 0 \Leftrightarrow \mathfrak{R} > \frac{1}{2}$  or,  $\sigma_a^V < 2\sigma_a^H$ . Now, if, as assumed, we have  $\sigma_1 \cong 0$ , then

$\mathfrak{R} = \frac{\sigma_a^H}{\sigma_a^V} \equiv \frac{R_H(h)}{R_V(h)} = \sqrt{4h^2 + 1}(\sqrt{4h^2 + 1} - 2h)$ . The condition  $\mathfrak{R} > \frac{1}{2}$  becomes

$\sqrt{4h^2 + 1}(\sqrt{4h^2 + 1} - 2h) > \frac{1}{2}$ . This is always true, *and must be expected in the case of a null*

*surface conductivity, otherwise our solution was false.* The real question arising here is: if  $\sigma_1 \neq 0$ , how far may we use that approximation (we do not ask here for the accuracy of the solution, but its existence)? The response is: as far as the data verify:  $\sigma_a^V < 2\sigma_a^H$ , since we have seen this condition is equivalent.

Next, we can retrieve the conductive layer conductivity by using  $\sigma_2 = \sigma_a^V \sqrt{4h^2 + 1}$ .

Now, do we make an important miss-estimation of  $(h)$  and  $(\sigma_2)$  by assuming  $\sigma_1 \cong 0$  if it is not true? We can provide a first qualitative response by considering the equation  $\sigma_a^V = \sigma_1[1 - R_V(h)] + \sigma_2 R_V(h)$  (and its equivalent for the horizontal mode).

If  $\sigma_1$  and  $h$  are small, the first term will be negligible. If  $\sigma_1$  is very small with respect to  $\sigma_2$ , it is also the case.

Notice that  $[1 - R_V(h)] = R_V(h)$  when  $h = \frac{\sqrt{3}}{2} \approx 0.87$ . In Potshini,  $h$  is expected to be smaller than this value. Although it will be interesting to push the error analysis further, let's consider that the error induced in  $(h)$  and  $(\sigma_2)$  are acceptable as long as, saying  $\frac{\sigma_1}{\sigma_2} \leq \frac{1}{20}$  after some numerical tests we did.

<sup>7</sup> We tried an analytical resolution: it leads to the search of a 8 degree polynomial roots. We did not complete this way but may be we'll do it later.

*BOX 5: solution from only ground based DV and DH data, while  $(\sigma_1)$  is known (provided by another experiment or indication)*

It is the case if we use the superficial conductivity as provided by surface small VES. In that case, first define  $a = \frac{\sigma_a^V}{\sigma_1}$  and  $b = \frac{\sigma_a^H}{\sigma_1}$ , and then compute  $\alpha = 1 - \frac{b-1}{a-1}$ . After some elementary calculations, one gets:

$$\begin{cases} h = \frac{\alpha}{2\sqrt{1-2\alpha}} \\ \sigma_2 = \frac{\sigma_a^V - \sigma_1(1-R_V)}{R_V} \end{cases}, \text{ with always } R_V(h) = \frac{1}{\sqrt{4h^2+1}}.$$

To use this method, one must ensure that simultaneously,  $\alpha > 0$  and  $1-2\alpha > 0$ . That is  $0 < \alpha < \frac{1}{2}$ . This leads to the condition:  $0 < \frac{\sigma_a^V - \sigma_a^H}{\sigma_a^V - \sigma_1} < \frac{1}{2}$ .

*Notice that, as far as  $\sigma_a^V$  and  $\sigma_a^H$  are theoretically derived (computed) by using a 2-layer model including  $\sigma_1$ , this condition is automatically fulfilled. What we state here is that this condition must be fulfilled by real data and externally imposed  $\sigma_1$  value, and this could be not verified for noisy data or if the value chosen for  $\sigma_1$  is aberrant, or simply if the 2-layer model is too far from reality.*

Let us consider that we are not too far from a two-layer reality. If  $\sigma_1 < \sigma_2$  (the real  $\sigma_1$ ), then we have automatically  $\sigma_1 < \sigma_a^V$  (because if  $\sigma_1 < \sigma_2$ , then

$\sigma_1 = \sigma_1(1-R_V) + \sigma_1 R_V < \sigma_1(1-R_V) + \sigma_2 R_V = \sigma_a^V$ , remembering that  $0 < R_V < 1$ ). Then, if we impose a known  $\sigma_1$  smaller than the real value, the computation will be possible.

However, whatever we do, we must check the condition  $0 < \frac{\sigma_a^V - \sigma_a^H}{\sigma_a^V - \sigma_1} < \frac{1}{2}$  before undertaking further computation.



BOX 6: attempt to solve the three equations by using Newton-Raphson's method.

Considering the system of equations given in BOX 3, it can be written as a system:

$\vec{F}(\vec{X}) = \vec{0}$ , and the Newton-Raphson method is justified in any numerical recipes book or easily found on internet. Remember that the method proceeds as follow: we go from an approximate (even very false) solution, that is  $\vec{F}(\vec{X}_0) \neq \vec{0}$ . We wonder: "what correction  $\Delta\vec{X}_0$  can we put to reach  $\vec{F}(\vec{X}_0 + \Delta\vec{X}_0) = \vec{0}$ ". Then we develop this equation to the first order of the Taylor series,

drop the Landau notation, and just keep:  $\vec{F}(\vec{X}_0 + \Delta\vec{X}_0) = \vec{F}(\vec{X}_0) + [\mathbf{J}_0] \Delta\vec{X}_0 \stackrel{\text{wanted}}{=} \vec{0}$ , where J is the Jacobian matrix of derivatives of  $\vec{F}$ . Then we have  $\vec{X}_1 = \vec{X}_0 + \Delta\vec{X}_0 = \vec{X}_0 - [\mathbf{J}]^{-1} \vec{F}(\vec{X}_0)$  and since we only develop at the first order, this define an iterative scheme of the form:

$$\vec{X}_{k+1} = \vec{X}_k - [\mathbf{J}_k]^{-1} \vec{F}(\vec{X}_k).$$

Under this form the Newton-Raphson method (NRM) is easy but doesn't include any consideration about:

- convergence of the process
- error analysis
- uniqueness of the solution.

In another hand, one could use a least-square method, that permits to introduce measurements errors and constraints, regularisation terms (the old Tikhonov theory) etc., just remember that the three equations to be solved here are equivalent to the ones we may derive by derivation of the objective function.

We did all that here to test Newton-Raphson's method to invert EM38 data. Except by imposing strong *a priori* information on  $\sigma_1$ , we got random convergence situation depending on initial values. We will understand why by using the last method (Bayesian inversion). Although we have now a more or less operational NRM code, we prefer to drop.

Other methods we did not test here could work: simulated annealing, homotopy and genetic algorithms, but none of them will describe fully the solution space, which Bayesian methods will do.

Let us do a first synthesis:

- In Potshini, a (shallow) simple two-layer electrical model seems to match the close soil condition; according to the electrical soundings and during the dry season, horizon A has a conductivity low, saying less that 5 mS/m;
- If  $\sigma_1 \ll \sigma_2$ , only two measurements are required to get the depth interface (h) and the second conductivity ( $\sigma_2$ ) according to BOX 4 formulae;
- If  $\sigma_1$  is given prior to EM38 use, only two measurements are required to get the depth interface (h) and the second conductivity ( $\sigma_2$ ) according to BOX 5 formulae;
- Solving classically the 3 equations with DV, DH, and DV at 0.5 m height is not satisfying, and it is very likely that no other least-square or usual inversion scheme (Tikhonov, simulated annealing, homotopy, genetic algorithms...) would work. This is due to the inverse problems usual difficulties: in a classical sense, the solution may not be unique, or, equivalently, the objective function shows complex patterns, local minima, and it is not

possible to find a single (and simple solution), despite the small number of parameters (three).

Several possible difficulties are inherent in our hypothesis, method and apparatus. First, the two-layer model cannot be satisfying with respect to field truth, there may be a more complex stratigraphy in the depth range to which the probe is sensitive. There may be non-horizontally stratified structure. And a known shortcoming of the EM38 is its drift worsening when it endures temperature variations (the drift shifts of all the readings by some constant). Note that this disadvantage has been reduced in more recent instruments by Geonics.

### Bayesian inversion of EM38 data

Finally we oriented our investigation toward Bayesian inversion. We recommend to the reader the synthetic paper by Tarantola and Valette (1982), Menke (1998), and the excellent books by Tarantola (1987, 2004)

<http://www.ipgp.jussieu.fr/~tarantola/Files/Professional/Books/index.html> -you can download it! (also see his excellent web page <http://www.ipgp.jussieu.fr/~tarantola/> ).

The way we use Bayesian inversion here can be found in Florsch *et al.* (2000) and Ghorbani *et al.* (2008).

Let us sum up the idea.

First it rests on the fact that the mathematical nature of the information we get on field data is probabilistic, due to the fact it is affected by errors. The expression “ $\bar{x} \pm \Delta x$ ” is used to say “x follow a Gaussian law with  $\bar{x}$  as mean and  $\Delta x$  as a standard deviation”. It is admitted that data generally follow Gaussian laws, and hence it is not required to provide any additional information (the Gaussian law being fully defined by its mean and first moment).

If we try to understand the informative structure of what we do when trying to retrieve natural quantities, we may introduce a diagram as the one depicted on Figure 9:

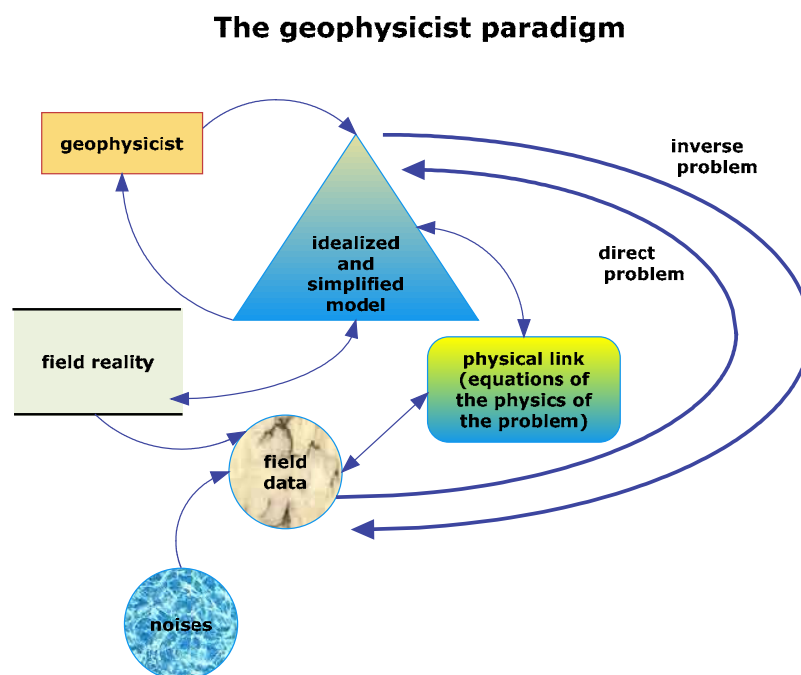


Figure 9

### **BOX 7: basics of Bayesian inversion**

Let  $\vec{d}$  be the data and  $D$  the data space,  $\vec{m}$  the model (parameters in the model space we name  $M$ ) and  $\vec{d} = G(\vec{m})$  the supposed exact physical law linking these quantities. ( $G$  is of course a vector with the same dimension as  $\vec{d}$ ). Often we have  $\dim(M) \leq \dim(D)$ , i.e. there are more data than parameters to be retrieved (notice that this condition is not required while using Bayesian inversion).

Let be  $\mu(\vec{m})$  the “null information” measure. Notice that if  $\vec{m} = (m_1, m_2, \dots, m_{\dim(M)})$  are all Jeffrey’s parameters, we have  $\mu(\vec{m}) = \frac{1}{m_1} \cdot \frac{1}{m_2} \dots \frac{1}{m_{\dim(M)}}$  (it is the case since conductivities and thicknesses are Jeffrey’s parameters).

Let  $\phi(\vec{m})$  the *a priori* pdf for parameters.  $\phi$  could be gaussian, or anything we want. In our case, it is the indicator function of the interval we are exploring to find the parameters, plus suitably normalized (i.e.  $\phi$  is uniform over these intervals).

We also suppose that the data are Gaussian, having a covariance matrix  $C_{dd}$

Then, the pdf of the parameters, which is also *the* solution of the inverse problem, is given by:

$$\text{pdf}(\vec{m}) = \frac{\phi(\vec{m}) e^{-\frac{1}{2}[\vec{d}-G(\vec{m})]^T C_{dd}^{-1}[\vec{d}-G(\vec{m})]}}{\mu(\vec{m})}.$$

It is the quantity we compute and plot in Bayesian inversion. Notice that we generally apply logarithm transformations to all Jeffrey’s parameters, and then it can be shown that  $\mu(\log(m_k)) = 1, \forall k$ , and this simplifies the computation by dropping this term.

Hence, taking into account the probabilistic nature of data, the question is: “**how to propagate the probabilistic information we have (with the data) into the space of models**”?

This is what Bayesian inversion does. Starting from the data space through the physical law, it carries the information into the parameter space in the form of probability laws of the parameters themselves. (See BOX 7 for a very few details).

We do not intend to develop that here in more details (see Tarantola’s books), but we show examples and shall use this approach. One advantage of this way is that it both performs the inversion itself and provides a fantastic investigation tool to find what is possible or not while dealing with a given inverse problem<sup>8</sup>.

<sup>8</sup> In this study, we consider that conductivities, resistivities, thicknesses are all “Jeffrey’s parameters”. Jeffrey’s parameter are

intrinsically positive parameters and follow non-informative probability measures of the form:  $\mu(x) = \frac{C}{x}$ ,  $C$  being a positive

constant (see Tarantola or Ghorbani to go into this question in depth). Usually, Jeffreys parameters follow log-normal laws, that is their logarithm follow Gaussian (normal) laws. For that reason and a lot of others,  $\log(\text{parameters})$  have to used in place of parameters themselves. By the way, it introduce in a natural way the positivity of the parameter as a constraint in the inversion.

Well, what we apply here in the Bayesian approach is just the computation of the unknown parameter law assuming some *a priori* information and overall the hypothesis that field data follows Gaussian laws. *A priori* information is also formed by a probability law. It can be the Gaussian or have any desired feature. For computational purpose, it is generally constraint into a “window” of parameter values, simply a given interval for each parameter. One can use that window alone and not add additional *a priori*.

Now let’s explain with an example supported by synthetic data. A data set we deal with has not redundancy: just three data  $\{\sigma_a^V, \sigma_a^H, \sigma_a^{V05}\}$  to recover three parameters  $\{\sigma_1, \sigma_2, h\}$ . We can consider that errors on EM38 are absolute or relative. Let us use absolute errors of 0.5mS/m and 5mS/m for our numerical experiment. Those are introduced as additional data in the code when computing. Let’s build a synthetic set of data, and to do that we take a representative model at Potshini, saying according to Figure 7:

$$\{\sigma_1 = 3\text{mS/m}, \sigma_2 = 30\text{mS/m}, h = 0.3\text{m}\}.$$

Logarithm in base 10 are:

$$\{\log_{10}(\sigma_1) = 0.4771, \log_{10}(\sigma_2) = 1.4771, \log_{10}(h) = -0.5229\}.$$

A direct calculation (see BOX 2) provides:

$$\{\sigma_a^V = 26.1523, \sigma_a^H = 18.2871, \sigma_a^{V05} = 16.4313\} \text{mS/m}.$$

All numerical applications are made with Matlab. The Bayesian code mainly provide a sampled description of the probability law of the three sought variables, that is the Probability Density Function:  $\text{pdf}_{\sigma_1, \sigma_2, h}(\sigma_1, \sigma_2, h)$ . Well, often that one does not provide normalized law, and then it is usual to name the law a “probability measure”.

This law **IS** the solution of the inverse problem. What can we do with it? Mainly estimate the probability for the parameters to be within a given set or interval, that is<sup>9</sup>:

$$\text{prob}(\{\sigma_1, \sigma_2, h\} \in I) = \iiint_I \text{pdf}_{\sigma_1, \sigma_2, h}(\sigma_1, \sigma_2, h) d\sigma_1 d\sigma_2 dh.$$

However, it is clear that neither the 3-dimensional pdf function nor the probabilities are easy to represent in mind. We could do slice of the pdf function, but the slices of pdf *are not* pdf, but just slices<sup>10</sup>.

For more practical use and plot, it is useful to deal with marginal probabilities. One may integrate over one of the variable, this provides the pdf of the two others. Or over two variables, this provides the pdf of one parameter. For instance:

$$\text{pdf}_{\sigma_2, h}(\sigma_2, h) = \int_{\text{whole}} \text{pdf}_{\sigma_1, \sigma_2, h}(\sigma_1, \sigma_2, h) d\sigma_1$$

Notice that Positive quantities like conductivity or thickness could not follow Gaussian laws since it would imply possible negative values! But data can, since the random behaviour of data is generally due to *additional* noise.

<sup>9</sup> I ignore here that we do not use these parameters, but their logarithms, actually! The transfer from that pdf to the pdf of the log involves a Jacobian determinant as in the change of variables in integrals. This is also dropped in the text for clarity.

<sup>10</sup> Nevertheless, in the paper by Ghorbani *et al.* we show 3-D representations.

(and the same for any couple of variables). We may continue, for instance to get the probability law for (h), one may use:

$$\text{pdf}_h(h) = \iint_{\text{whole}} \text{pdf}_{\sigma_1, \sigma_2, h}(\sigma_1, \sigma_2, h) d\sigma_1 d\sigma_2 .$$

Geophysicists or their chiefs often want single parameter results. “Well beautiful, but what IS the value for h”. Answering this question makes also the connection with more traditional least-square method<sup>11</sup>. The only thing to do is to perform the moments of the one-dimensional pdf. For instance, a response relative to (h) would be its first two moments, i.e. the mean and the variance:

$$\bar{h} = \int x \cdot \text{pdf}_h(x) dx \quad \text{and} \quad \text{var}(h) = \int (x - \bar{h}) \cdot \text{pdf}_h(x) dx .^{12}$$

Let us now shows the two-by-two solution pdf, first assuming a small error of 1 mS/m.

Zooming on results provide the following explicit Figure 10. Clearly means match the input model parameters (remember that Logarithm in base 10 are:

$$\{ \log_{10}(\sigma_1) = 0.4771, \log_{10}(\sigma_2) = 1.4771, \log_{10}(h) = -0.5229 \} .$$

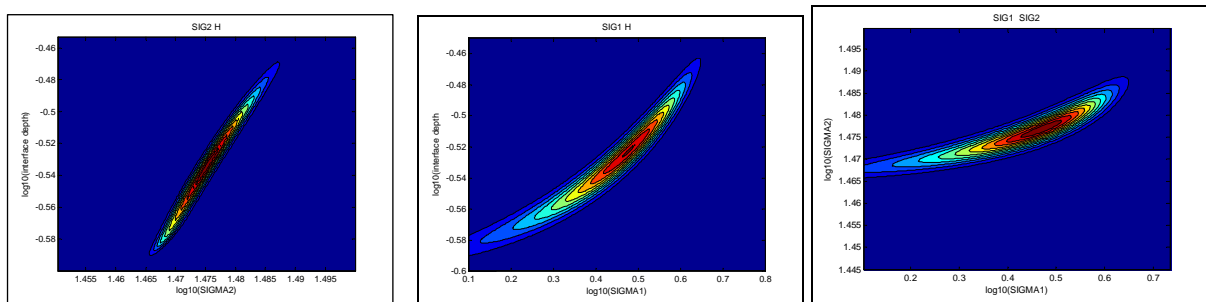


Figure 10

If we transform log-means in standard parameters, one finds:

$$\begin{cases} \tilde{\sigma}_1 = 2.61 & (\text{original} = 3) \\ \tilde{\sigma}_2 = 29.9 & (\text{original} = 30) \\ \tilde{h} = 0.294 & (\text{original} = 0.3) \end{cases}$$

Now let us make a more realistic numerical experience. We *introduce a systematic error*. It is what occurs with EM38 if we assume that the reading is correct, while *it had been badly calibrated, or had drifted*. We change:

$$\{ \sigma_a^V = 26.1523, \sigma_a^H = 18.2871, \sigma_a^{V05} = 16.4313 \} \text{ mS/m}$$

into the drifted set (and rounding to introduce also a light random noise):

$$\{ \sigma_a^V = 24.1, \sigma_a^H = 16.3, \sigma_a^{V05} = 14.4 \} \text{ mS/m} .$$

It is necessary to provide realistic error bars. Being realistic let's put an error bar that could correspond to a security coefficient for the field possible instrument drift, let's set error=4 for that apparatus (it is what I would employ in practice if I was not sure of the control of the instrumental drift). We can see that the second conductivity and the depth are well defined. However, only the

<sup>11</sup>Least-square methods generally provides one or several maxima of the pdf we deal with here... when they work

<sup>12</sup> Warning, it is not supposed that the pdf is unimodal!

upper limit of  $\sigma_1$  is clearly defined, while it can be very low. It exactly means that a very high resistivity of the first layer *is* compatible with the data and the error bars.

One can also plot now the probability laws of each parameter (there are not normalized here), on Figure 11a and Figure 11b.

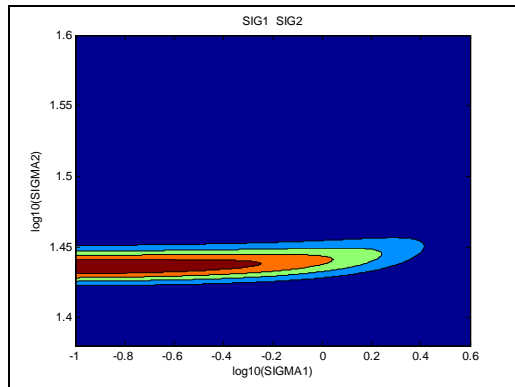


Figure 11a : two-by-two marginal probability laws for the 2 layer model parameters. Notice these laws show that very low  $\sigma_1$  are possible. More exactly, if you choose a point within the solution plotted in red, the theoretical data you will derive from those points by a direct calculation will fit the effective data.

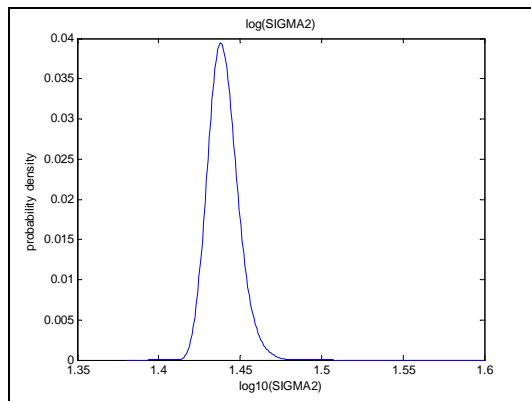
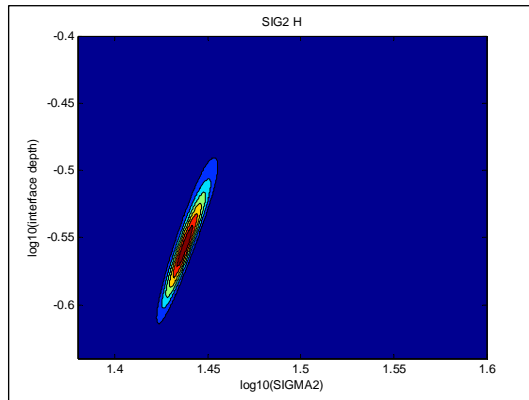
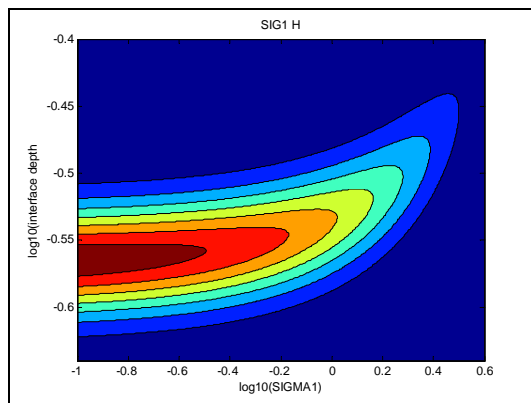
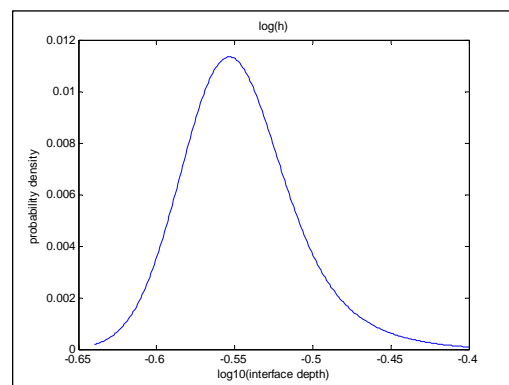
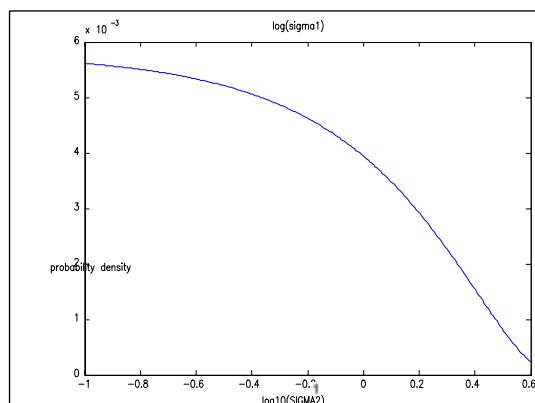


Figure 11b : one-by-one marginal probability laws for the 2 layer model parameters (3 parameters).

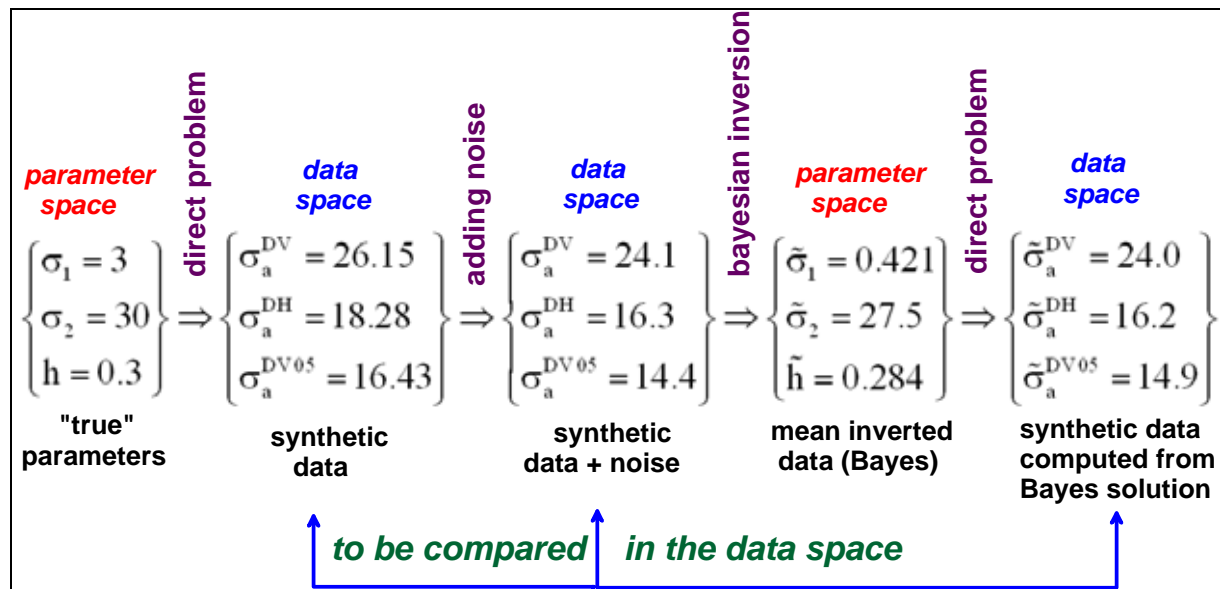


The retrieve single values, one first compute the mean of the log pdf, and then take the power of 10. This leads to the estimated value in mS/m:

$$\begin{cases} \tilde{\sigma}_1 = 0.421 & (\text{original} = 3) \\ \tilde{\sigma}_2 = 27.5 & (\text{original} = 30) \\ \tilde{h} = 0.284 & (\text{original} = 0.3) \end{cases}$$

Those results are fine for  $\sigma_2$  and  $h$ . It seems less good as far as  $\sigma_1$  is concerned. *Actually, one has to understand that it is fine!* Indeed, the result of the inverse problem is not this value, *but the whole pdf*. It means exactly that the *observed data* are representative of possible values of the parameters *as shown on this pdf*<sup>13</sup>. The above mean for  $\sigma_1$  is correct, closer to the mean of the possible value *set* compatible with the data than the original value is itself! That is, given the data, it is at the barycentre of the possible parameter value set. Their pdf can be used to compute the probability for a given parameter to belong to any given interval.

To conclude let's compute the *theoretical data* following the idea in Figure 11. We summarize in the following chain:



We see that the method is robust (in fact Bayesian inversion cannot be unstable!) and retrieves the parameters in a way the re-computed data fit the observed data (including noise).

Now let's test on some *real data*.

### Ravine area with EM38

The so-called "Ravine" area is the one at the south part. All results are shown on Figure 12.

Unfortunately, the people making the measurements had a poor experience in manipulating this EM38. Although they did not make any special mistake, they were not aware of the level of

<sup>13</sup> I can suggest here to read Tarantola's paper on the philosophy of data:  
[http://www.ipgp.jussieu.fr/~tarantola/Files/Professional/Papers\\_PDF/NaturePhysicsTarantola.pdf](http://www.ipgp.jussieu.fr/~tarantola/Files/Professional/Papers_PDF/NaturePhysicsTarantola.pdf)  
 See also <http://www.stats.org.uk/bayesian/ScalesSnieder1997.pdf>, at least for fun.

attention required when we use it for purely quantitative purpose. Let us be more precise, this not to criticize, but in order to improve the next campaign.

### **BOX 8: how to get good data with the drifting EM38?**

One calibration is done by handling the probe above one self, and to adjust one button until a ratio of 2 (between the DV and the DH mode) is exactly reached. This is based on a far field property of the apparatus-ground coupling. This adjustment allows to remove the offset that may result from the drifting. If done after a warming delay, it remains OK unless the temperature changes. Generally, the temperature changes! Then one has two alternative modes of working: 1) we redo the calibration. But what about if we do not redo it perfectly? We introduce an additional offset! 2) we let it drift during the day (*with the power on at all time of the day!*), but we regularly go to *the same location and position* and one *take note of the drift, in the same way we could do in magnetic prospection*. After that, in the lab, one applies corrections to remove the drift.

This second procedure is definitely superior to the first one as far as the data are to be used for inversion. Any other method introduces unwanted offsets in the data<sup>1</sup>. We strongly recommend following it.

*Notice that in the more recent Geonics EM38, the drift problem had been reduced.*

It followed that only about 50% of the data can be inverted, that is, fulfils the condition given in BOX 5.

The arrow A points at a location where some negative values of DV conductivity exist. It reveals the very probable presence of metallic artefacts. We are very far in this part from the layered model, and inverting data using this hypothesis is of course not valid.

Arrow B points a confined more or less linear structure not visible on the EM31 map. Hence, it must be superficial. Correlation must be, later, done with the topography. Here also the layered model is not valid, and the area is rejected by the conditioning equations.

C arrows show a jump in the data, that is a spatial (and hence temporal) offset! Does it concern the lower part or the upper part of the map? It is impossible to state! Notice that when dealing with this set of data, a slighter offset has been detected in  $y=50$ , probably due to the time delay to change the decametres in operation (it is hardly visible on these figures).

The arrow D points an area where values can be inverted, but seem unrealistic.

And finally if we look to the part of the maps that seem fair, we observe a correlation between the interface depth and the lower layer conductivity. This is possible, but is it probable? Firstly, we would suppose a kind of equivalence, similar to those we deal with in DC prospection. We think it could be the case: the deeper the interface to reach the conductive layer, the more conductive you must have to compensate the depth (for a fixed datum). *However* this behaviour is spatially organized. An artificial correlation should be more random. And finally, the inverted quantities are also correlated with the raw data. We cannot exclude the possibility that the conductivity of the lower layer is higher in the areas where the interface is thicker, for the reason that it is deeper, and then wetter too! It could be verified by excavating.

Why such an amount of data that cannot be inverted? In some location (A,B) the 1-D model is not the good one. It could be the same problem on other location, since numerous termite nests are located here and could be associated with important but shallow heterogeneities.

In conclusion on that first inversion, let us consider that it could be redo with much more caution, and since a new EM38 is awaited, by using the new one. However, this first data exploration enforces our confidence into the methods given here to try recover horizon A thickness at least in selected zones where it is not disturbed by and another ground conformation than the layered one.

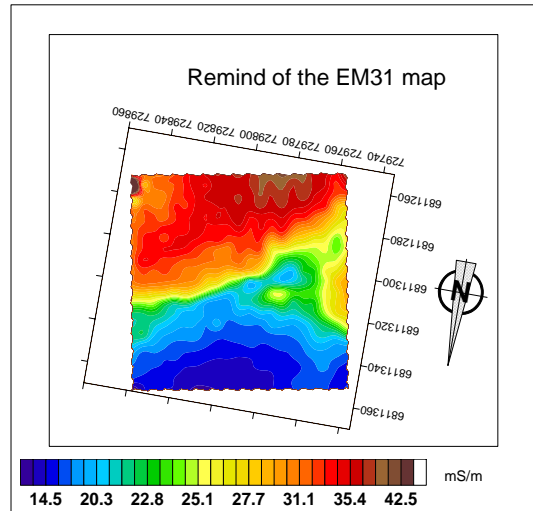
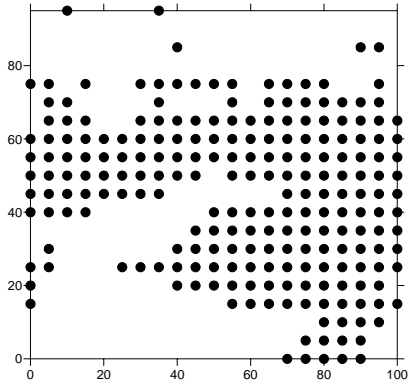


*What a beautiful country*

Analytical Inversion of EM38 data,  
 DV and DH modes used.  
 The conductivity of the first layer is forced à 2 mS/m.

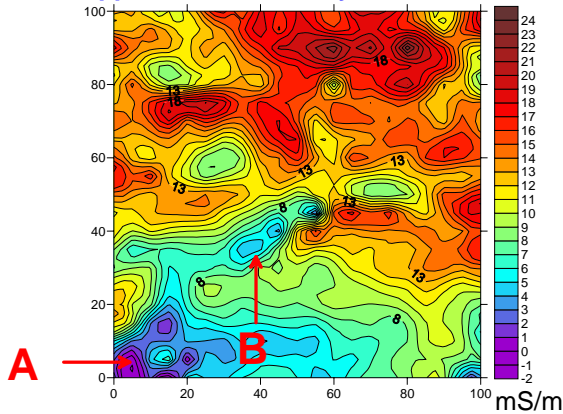
Figure 12

Data which can be inverted

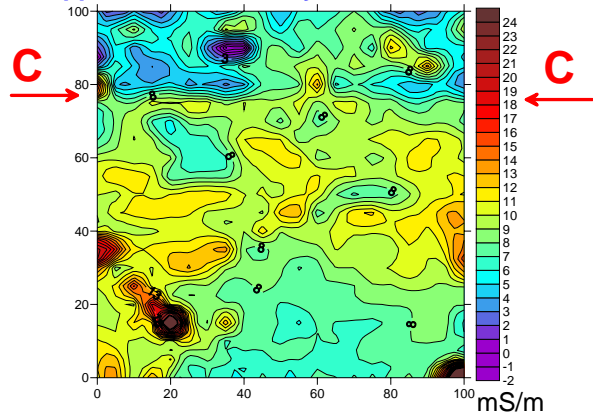


Red arrow labels are  
 discussed in the text.

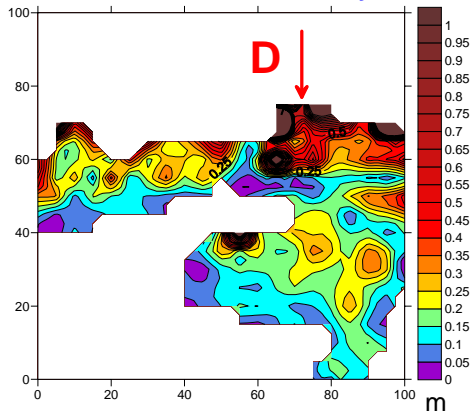
Apparent conductivity Vertical mode



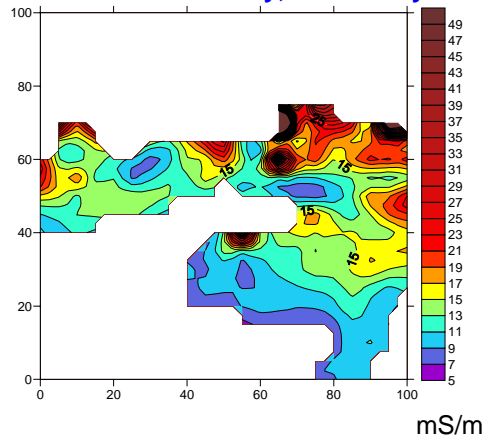
Apparent conductivity Horizontal mode



Inverted tickness, first layer

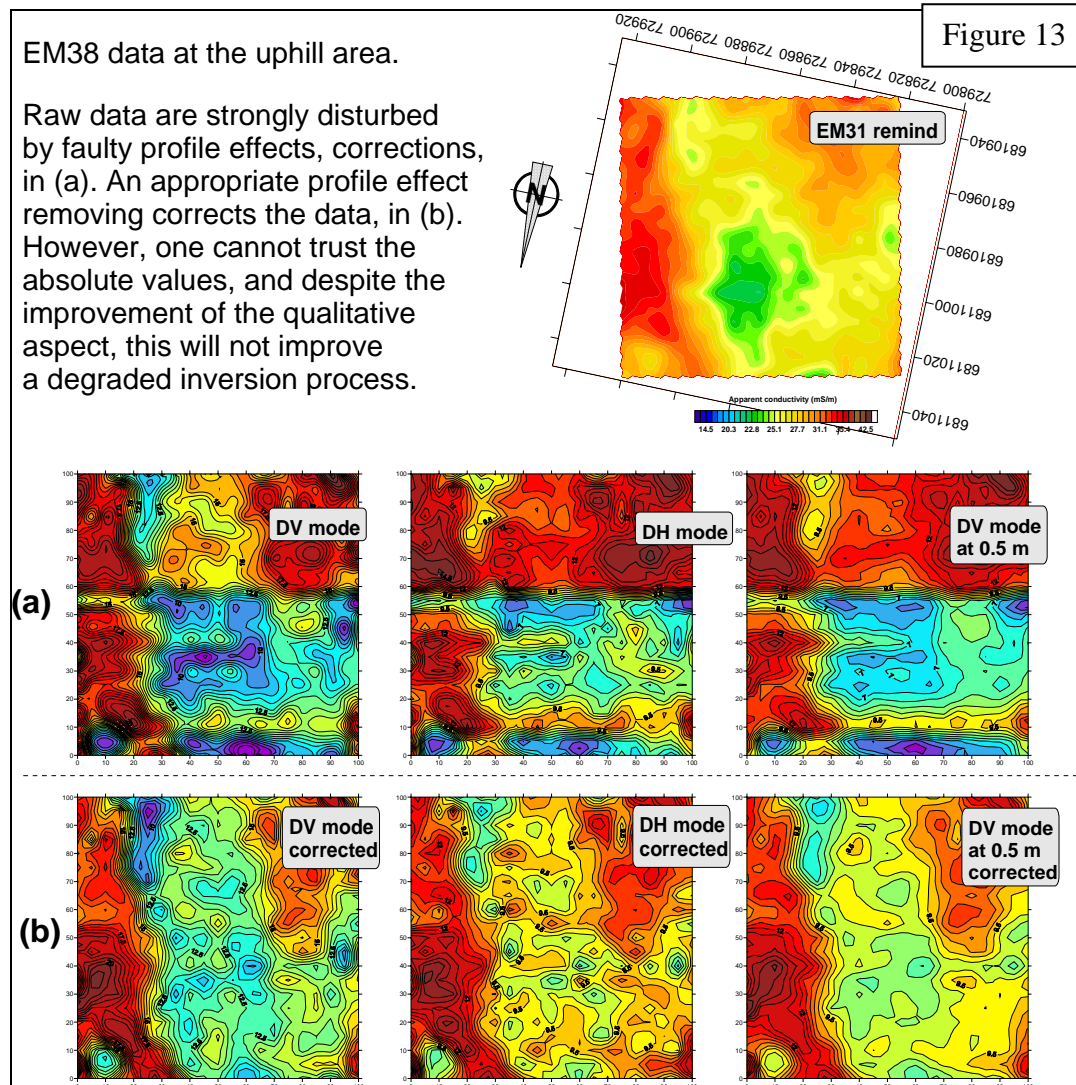


Inverted conductivity, second layer



## The “upper/uphill” zone.

Let’s now deal with the second 100mX100m quadrat. It will be short since the profile effects, parallel to the x axe, are worse than on the Ravine map, as we can see on Figure 13. A 5mX5m grid has been used.

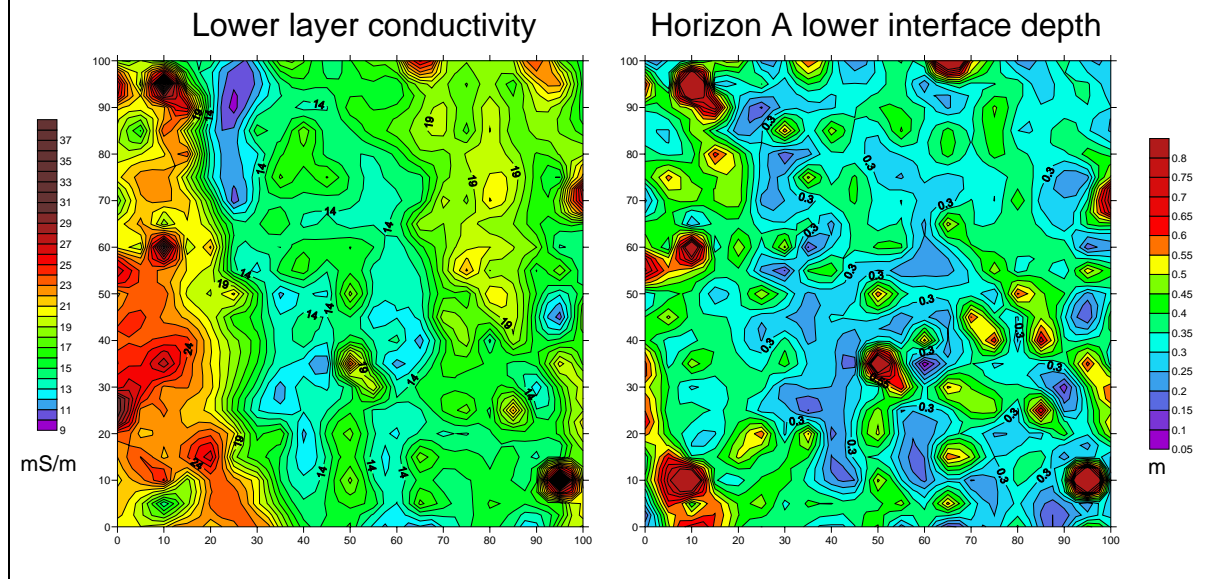


We first apply the previous analytical method, dropping the measurement in DV mode at 0.5 m height... just to see. We adopt a first layer conductivity of 3mS/m.

A good surprise, only 0.68 % of the points are rejected! (That is: 3 points). The result is shown on Figure 14 below:

EM38 uphill: analytic inversion based on DV and DH modes only and assuming a first layer of 3mS/m conductivity

Figure 14



All values are realistic, except a very few outliers. *A preliminary spatial low-pass filtering would certainly have smoothed these maps. We'll try another time.*

However, I would not put this in a published paper since the profile effects have been artificially removed (just by imposing the same average to all profiles parallel to the x-axis).

Let's try to invert the uphill maps by using Bayesian inversion. Normally, at *each* point, the whole Bayesian inverse calculation is performed. But here we have 441 point, (the grid is 5mX5m), and it is not practically possible to plot 441\*6 histograms as we did previously with the synthetic example<sup>14</sup>. So what we do is to provide means and standard deviation.

We continuously keep in mind that the data are probably shifted by the cosmetic profile effect removing!

Now for the same data let us comment on Bayesian inversion. Main results are shown on Figure 15. **The error on data has been set at 3 mS/m** (high enough to take into account the recipes to reduce profile effects).

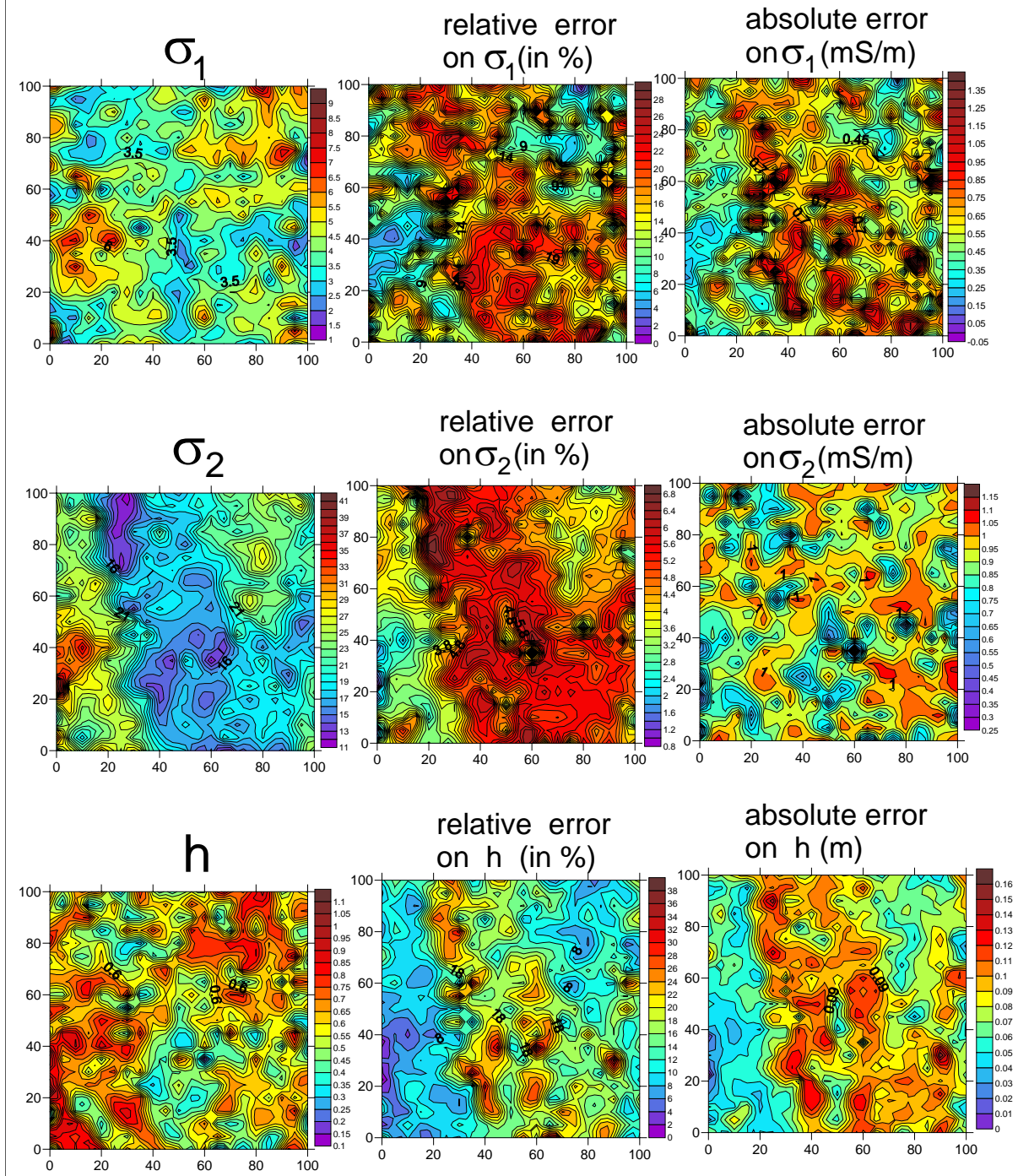
First keep in mind the window where the parameters are explored. *This window implies that parameter a priori information are uniform laws (constant probability) over the corresponding interval, and vanishes outside these windows. Hence, a parameter CANNOT be found outside.* It is one of the meaning of the Bayesian inversion: *what about the parameters once the a priori information is put inside the problem?* Hence you have this philosophy: before measuring, you have *a priori* information. By measuring, you introduce additional information to be combined with the previous knowledge. This is the Bayesian paradigm! Notice that errors are also to be understood in that frame: parameters cannot be outside the explored intervals, and this is a subsequent consequence of the choice of this kind of *a priori* intervals.

Let recall these intervals:  $1 \leq \sigma_1 \leq 10 \text{ mS/m}$ ,  $10 \leq \sigma_2 \leq 100 \text{ mS/m}$ ,  $0.05 \leq h \leq 1 \text{ m}$ .

<sup>14</sup> With Matlab which is slow with respect to C++ or F77/F90 languages, processing one point needs a few minutes.

# Bayesian inversion of EM38 data in the uphill area

Figure 15



This *a priori* information is continuously combined with the structural one, which is the supposed 2-layer structure. In the Bayesian language, this means that the results above have to be read: “here are the parameter values assuming the 2-layer structure is valid and assuming they lie in the given intervals”.

Now it is of great interest to have a look to some detailed inversions, that is the pdf of inverted parameters. This could be done for the whole map (441 points), but would be paper consuming! Let’s take only a few examples. I choose points: (20,20), (40,40), (60,60) and (80,80). All quantities are tabulated below:

Coord.		Field data			Recovered parameters and corresponding errors					
x	y	$\sigma_a^v$	$\sigma_a^v$	$\sigma_a^v$	$\tilde{\sigma}_1$	$\tilde{\sigma}_2$	$\tilde{h}$	Err ( $\tilde{\sigma}_1$ )%	Err ( $\tilde{\sigma}_2$ )%	Err ( $\tilde{h}$ )%
20	20	18.58	12.39	12.49	4.4	28	0.66	7	3	5
40	40	13.35	9.98	9.11	4.2	17	0.47	17	4	13
60	60	12.43	9.72	8.82	5.1	16	0.52	15	5	15
80	80	13.33	11.34	11.48	5.5	27	0.83	5	3	4

The following Figure 16a, 16b, 16c and 16d provides all the pdf (only two two-by-two graphics are required to plot the full information):

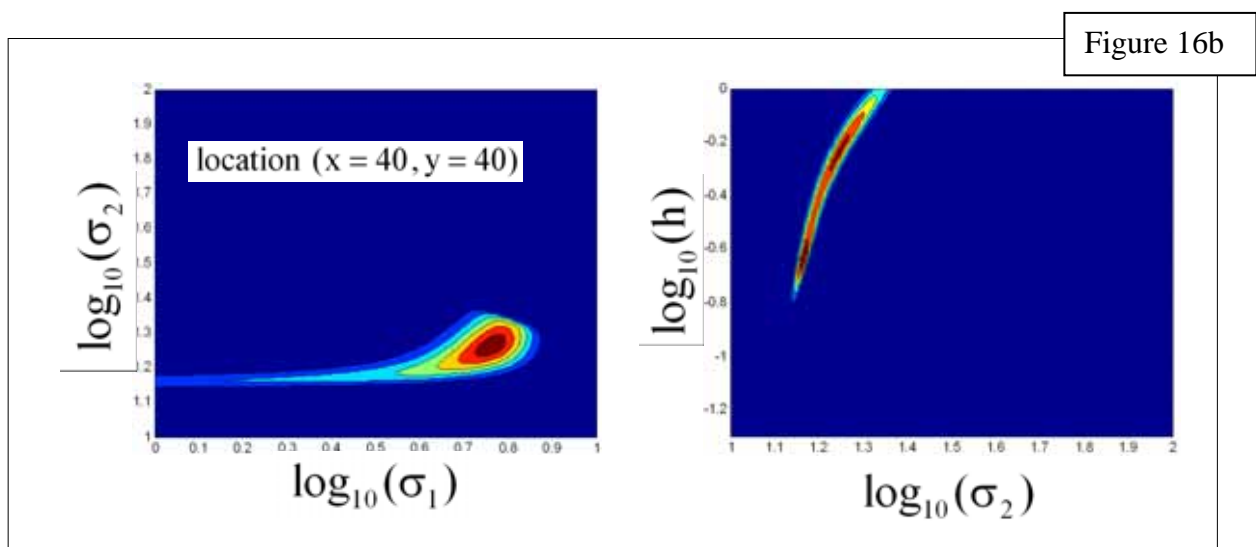
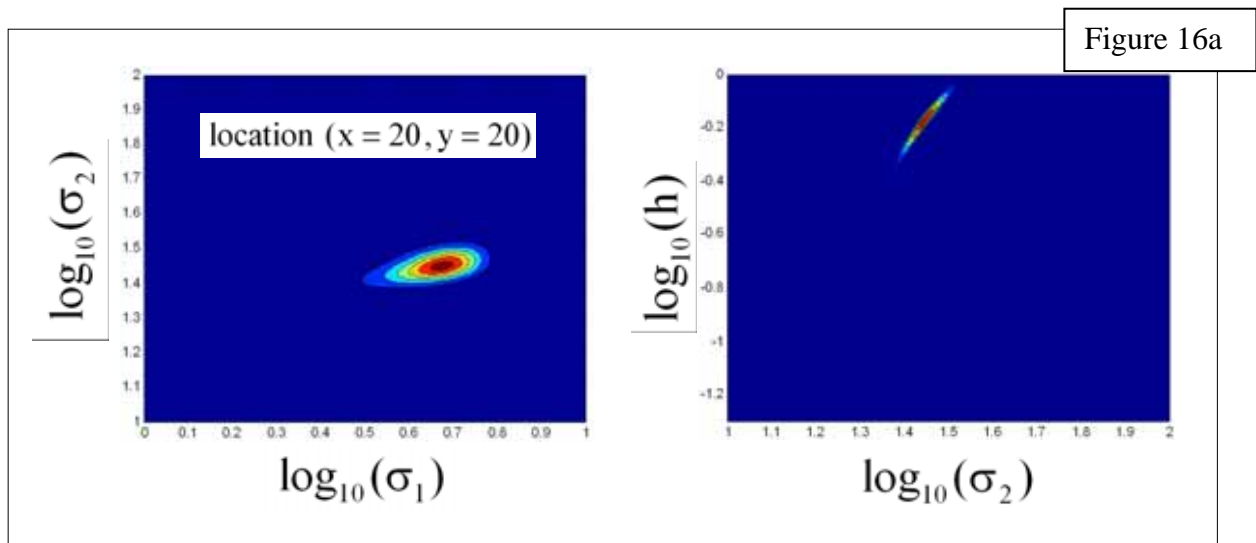


Figure 16c

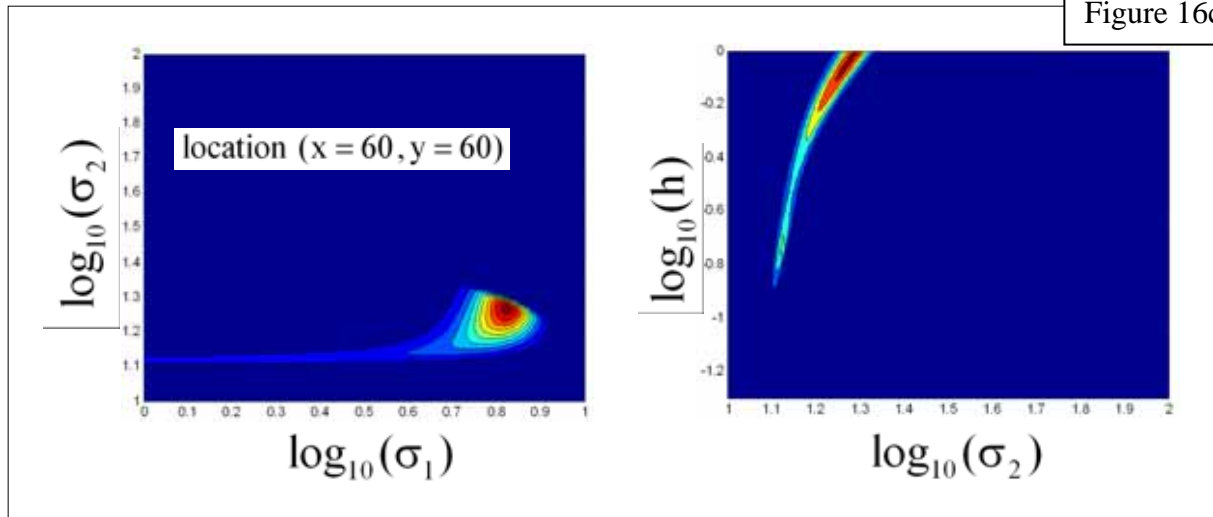
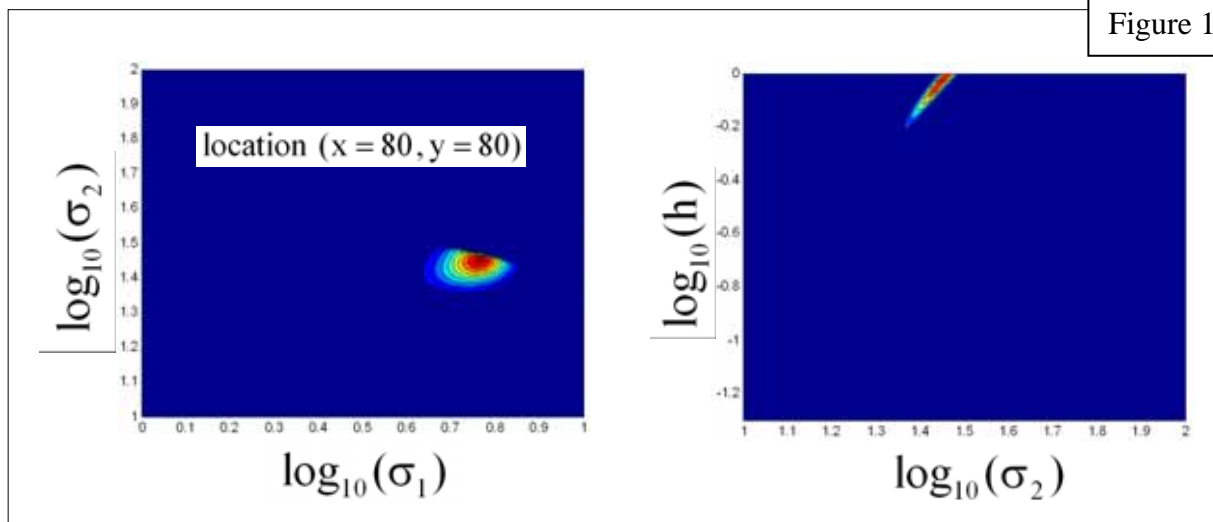


Figure 16d



On the right figures, we can observe a systematic trade-off/correlation (“equivalence phenomenon” as geophysicists say) between  $\sigma_2$  and  $h$ . The solution is cut by the  $h$  upper limit as defined by the *a priori* information. It means that it is possible that, in the frame of the 2-layer model, the *a priori* information is badly chosen by the geophysicist<sup>15</sup>.

The patterns in the left figures seem to have been cut. These results from the boundary applied to  $h$  itself while choosing the *a priori* intervals.

Of course this inversion can be used to investigate more deeply the properties of the solution, or to extend or limit the investigation in the parameter space.

<sup>15</sup> It is *impossible* to define an inverse algorithm without a part of subjectivity. If you use simple least-square, it means that you *assume that the data are Gaussian*. If you use regularization method, you introduce generally a Gaussian *a priori* law. Since you choose a method, you are involved as a human being!

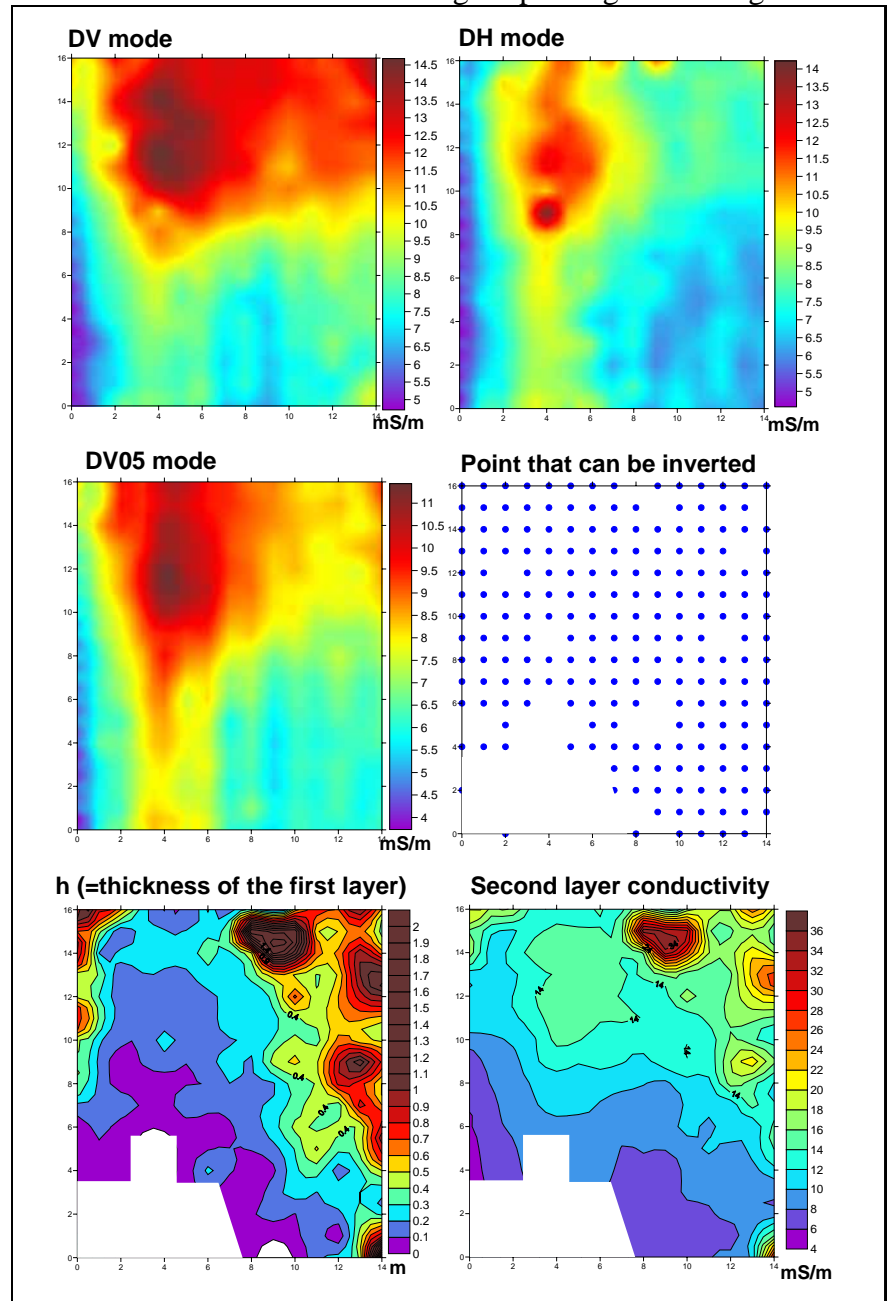
## The B71 tree area.

This study was a first test to know if we could see, through geophysical measurement with EM38, the impact of the presence of a tree on the soil. It is a small area around a tree named B71. The tree is located exactly in the middle of the studied area (14m\*16m). The grid is 1mX1m.

Profile effects seem properly reduced by the drift correction procedure.

We first do the inversion by using only DV and DH and assuming a first layer conductivity of 3 mS/m. We get 16% of the points that cannot be inverted. Resulting Maps are given on Figure 17.

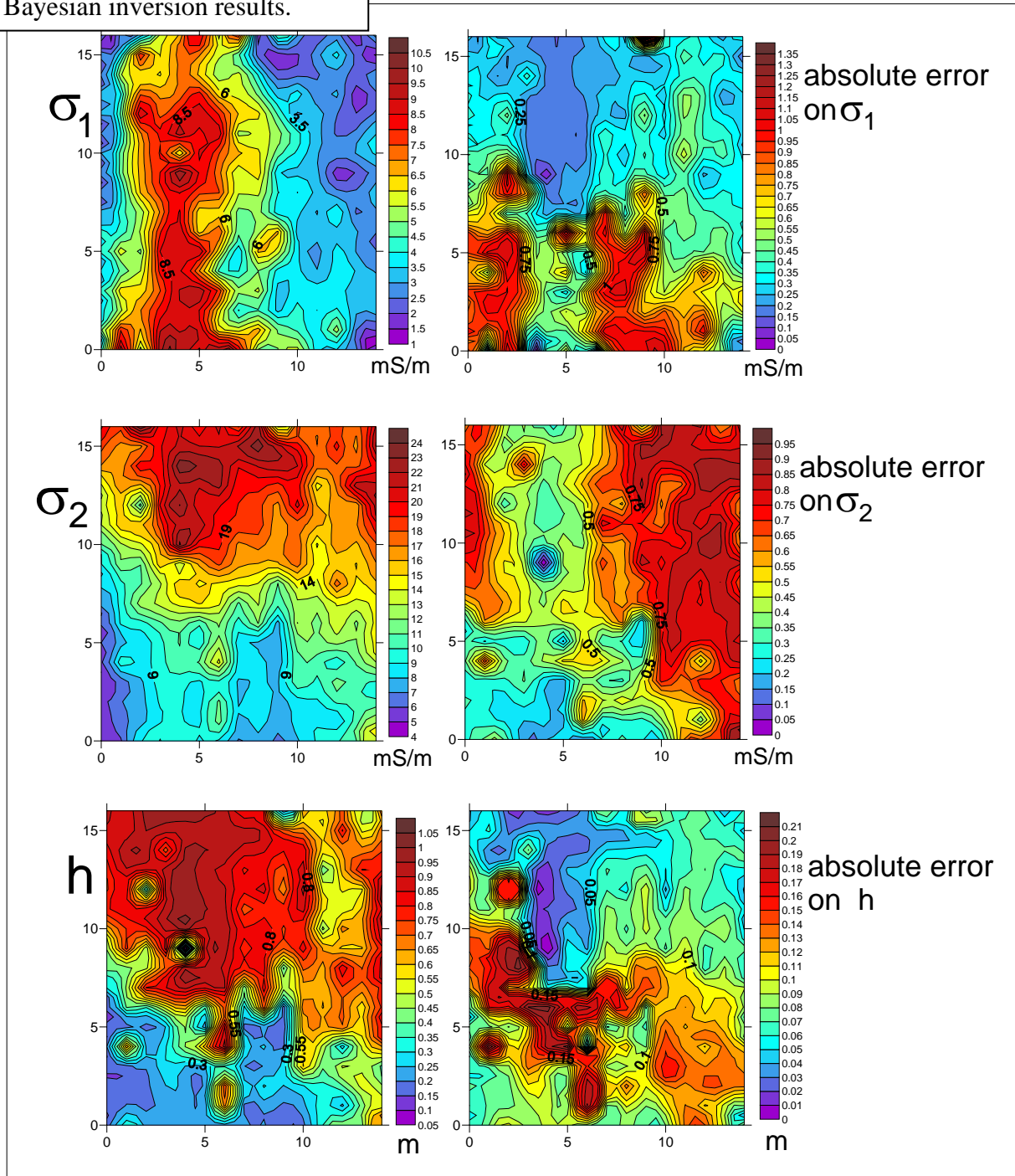
Figure 17 : B71  
Two parameters  
analytical inversion



When using now the Bayesian inversion, we supposed that the measurements error was 2 mS/m<sup>16</sup>. We get the following results, on Figure 18:

<sup>16</sup> The lower error that can be probably and reasonably reached on that device is 1mS/m. It could be better with the new systems now available from Geonics.

Figure 18 : B71  
Bayesian inversion results.



These maps show interesting features. Firstly,  $\sigma_1$  and  $\sigma_2$  are uncorrelated. Secondly, we notice a partial correlation between  $h$  and  $\sigma_2$ . Thinking forward they do not increase in the same manner at the upper part of the map. Actually one must keep in mind that the deeper, the wetter. Hence, while the interface gets deeper, the observed second layer is deeper too, and wetter, and consequently more conductive.

The south part (upper part also) of the area seems reflecting an accumulation of water due to a deeper A horizon which could be due, in part, to the presence of the tree. The accumulation of

sediment in the upper part and the loss of sediment in the lower part is well known in erosion processes. However, after analysing the data of EM31, the tree B71 appears to be in an area with a high contrast of conductivity between the north and south of the studied area. This is explained mainly by geological features. Thus, the impact of the tree on the soil conductivity is itself probably hidden by this feature. Another tree located in a geologically homogeneous area would be better to try to see any effects on the soil conductivity.

Of course, as all results in this “blind” study, verification soundings must be undertaken on the field to check all these hypotheses.

## 2. Vertical Electrical Soundings (VES)

*The location of VES are given in ANNEXE 4.*

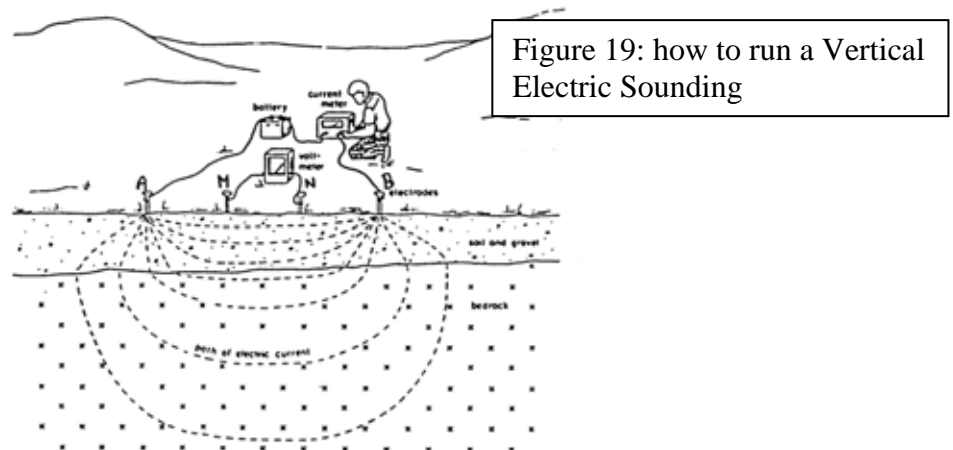
We did three sets of VES:

- 1) a first one with only one sounding “SEV01”, just to see
- 2) a set on well defined conductive or resistive areas defined from the EM31 map. These are SEV02 to SEV08. This is the proper way since it prevents doing soundings which are devoted to tabular layered ground too closely to lateral resistivity transitions
- 3) a set of VES along the toposequence, named TS1 to TS8

Let’s quickly recall what VES are aimed to<sup>17</sup>.

A VES consists in sending electrical currents into the ground by using two current electrodes C1 and C2 and by measuring the resulting voltage between two receiving electrodes named P1 and P2<sup>18</sup>.

Various layouts are used, having relative advantages and disadvantages. We use here the traditional “Wenner –  $\alpha$ ” array, that is the four electrodes are equi-spaced by a distance  $a$  and in a straight line. It is shown on Figure 19:



(from [www.argenco.ulg.ac.be/GEO3\\_Hydrogeologie/pdf/These\\_Rentier/14\\_AnnexeB.pdf](http://www.argenco.ulg.ac.be/GEO3_Hydrogeologie/pdf/These_Rentier/14_AnnexeB.pdf))

If we suppose that the ground is homogeneous, a simple formula gives us the resistivity from the current  $I$  (into C1 and C2) and the difference of potential between P1 and P2,  $\Delta V$ . It is:

<sup>17</sup> The reminders given in this report are for non-geophysicists!

<sup>18</sup> C for current and P for potential. The French tradition uses A and B for current and M and N for the potential.

$$\rho = 2\pi a \frac{\Delta V}{I} = K \frac{\Delta V}{I}.$$

(K is the so-called geometric coefficient and varies according to the kind of array). It is easy to understand that the larger the array, the deeper the investigation. Hence, the idea of the VES is to increase the characteristic distance a (for the Wenner array) and to derive the apparent resistivity which will concern more and more thick and deep layers. That why it is called “vertical” electrical “sounding”.

The VES is plot as a function of the logarithm of the apparent resistivity versus the logarithm of a.

Here are some features of the method:

- it follows multiplicative invariance, that is the curve of two homothetic models (resistivity or geometry) are superimposed on a log-log scale. We do plot curves on such a double scale;
- the VES is fundamentally a one-dimensional procedure, and hence a good interpretation relies on the validity of a one-dimension hypothesis: that the resistivity only depends on z (what the geophysicist call a “tabular structure”)
- globally the apparent resistivity VES curve follows (and looks like) the variations of the resistivity with depth; but remember the log-log behaviour: a layer of thickness T at a depth D has the same influence on the curve as a layer with thickness  $x \cdot T$  and depth  $x \cdot D$  while a layer with a fixed thickness will disappear when its depth increases without scale compensation;
- the VES curve is definitely much smoother than the real resistivity sequence; hence the details in layering are not visible
- the method is subjected to numerous limitations; for instance: about a (relative) conductive layer, only the ratio of thickness to resistivity can be retrieved – and for a resistive one, it is the product; or, when a layer of intermediate resistivity is embedded between one more resistive and another more conductive, one can miss it if it is not thick enough
- unless the VES curves become almost horizontal at its right end, the last layer is badly constrained, as far as its resistivity is concerned, but the depth of the last interface is generally not badly determined.

And so on; interpreting resistivity curves is a job in itself (the geophysicist’s one).

1) First set: the SEV01 alone.

By a bad chance it is done on a transition zone, so that the tabular hypothesis is not valid. Nevertheless it provides a first insight that is useful. It shows a first resistive layer of almost  $200 \Omega \cdot m$ , 50 cm thick, which could correspond on the top soil dried by both herbs pumping and direct evaporation (O+A horizons?). It is followed by a very conductive layer. Equivalence analysis shows that the parameters of this electric layer can be between  $8 \Omega \cdot m$  with a 30 cm thickness to  $20 \Omega \cdot m$  with 90 cm (respectively according to equivalence laws). I adopt  $12 \Omega \cdot m$  and about 50 cm as a mean probable value. This layer is humid and clayey. Beneath we find a more resistive layer ( $50 \Omega \cdot m$ ) and it becomes more and more resistive with depth, probably just by the decrease of the weathering.

2) SEV02 and SEV06 have been made on resistive patches on the EM31 map. Underneath SEV06, a conductive layer undoubtedly exists and causes the general decay of the resistivity curve; however it is at a 5 m depth at the detection limit for the Slingram device. This conductive horizon may be interpreted as a residual water sheet overlying a less permeable medium. The vadose zone is relatively dry, and in fact there may be a good drainage that makes this area resistive. The “apparent” bedrock is at about a 10 m depth. SEV02 is more complex. The shallow conductive layer is too thin to influence the EM31 value a lot. The EM31 conductivity is about 20 mS/m that is  $50 \Omega \cdot m$ .

Let’s take this SEV02 case to study two possible solutions, saying I1 in which we accept a shallow conductive layer occurrence, and another one I2 where we consider that the small undulation in the curve could be do to a lateral affect (the medium is not tabular and we could have this artefact).

The measured conductivity on the EM31 map gives conductivity between 18 and 20 mS/m at SEV02 location.

Here are the two solutions:

I1 with the shallow conductive layer, Figure 20a

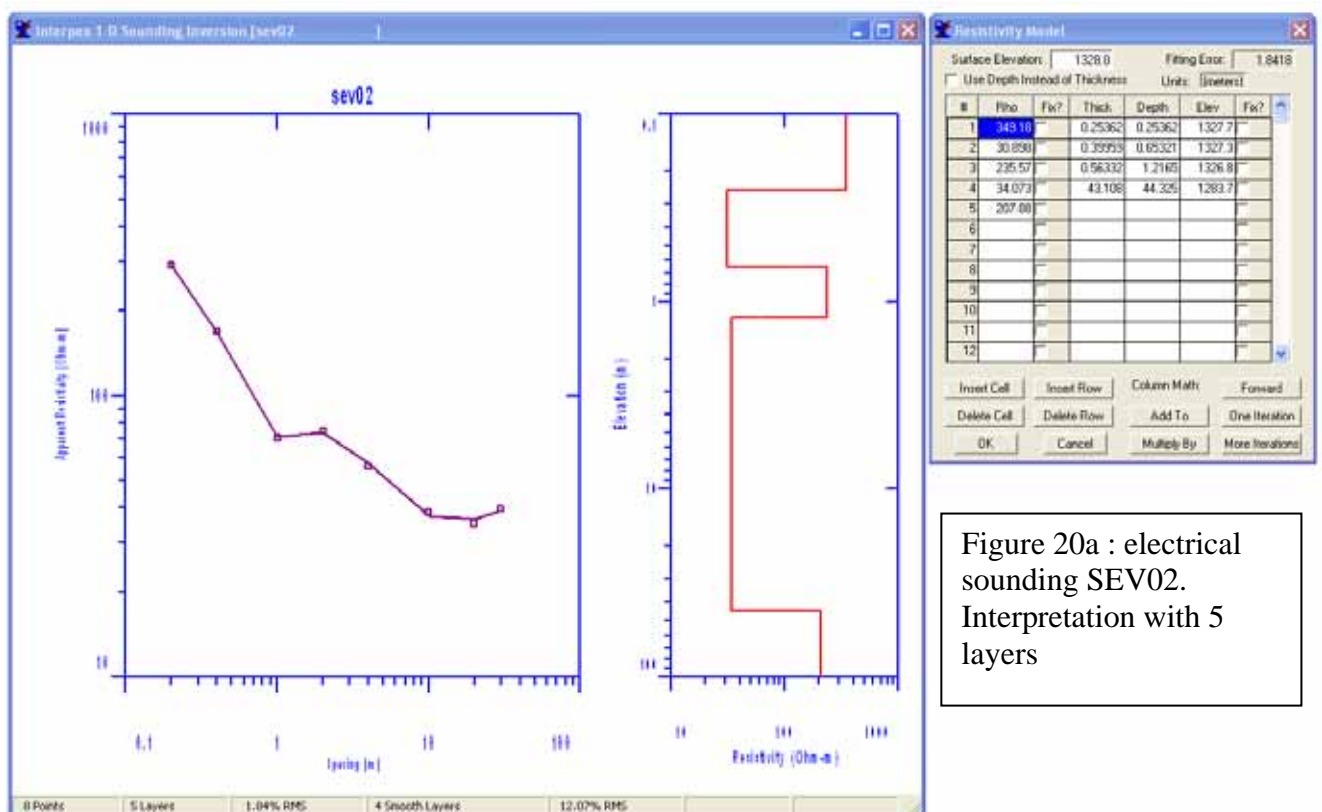


Figure 20a : electrical sounding SEV02. Interpretation with 5 layers

And here I2 with a simpler model, Figure 20b.

Now using the formula which give the conductivity for EM31 (EXTRA 2), we calculate the expected conductivity from these two models. It leads to 24 mS/m in the first case, but 20 mS/m in the second case. It tends to prove that the S2 interpretation is better than the S1 when comparing with EM31 values.

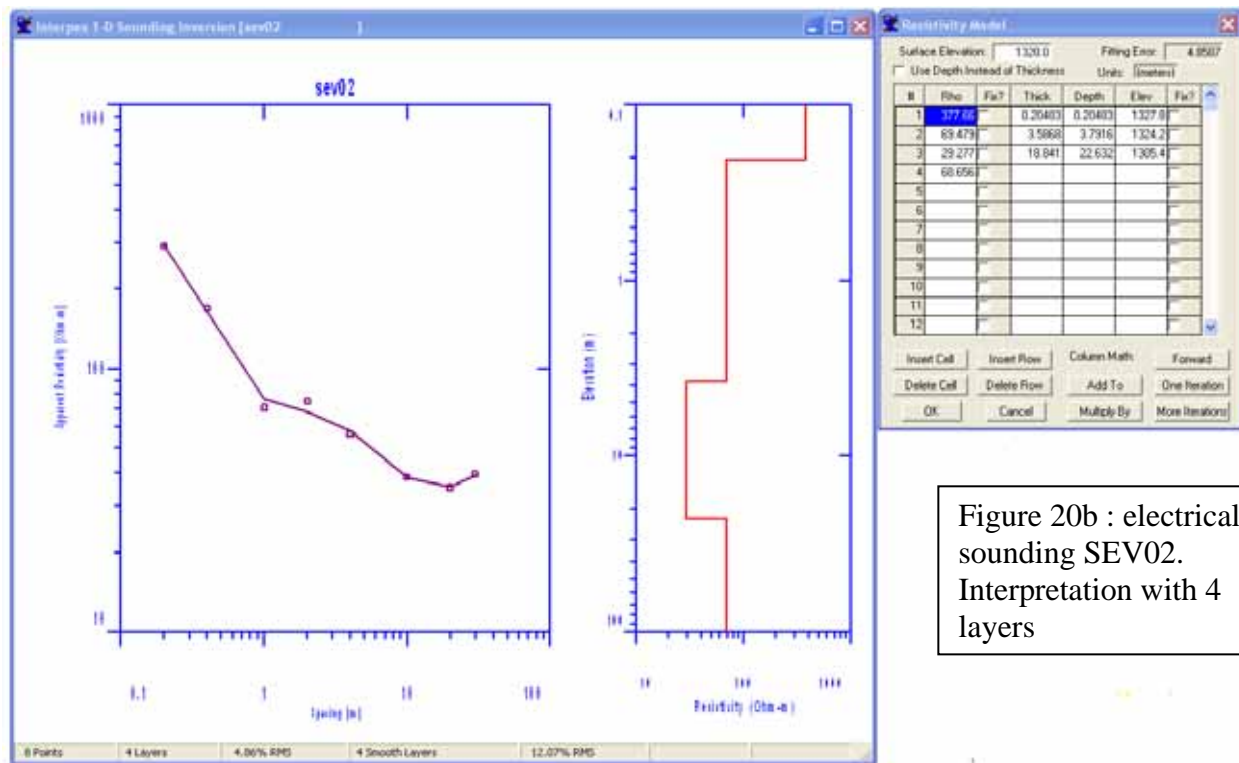


Figure 20b : electrical sounding SEV02. Interpretation with 4 layers

Now consider SEV06 which is also ambiguous. Here are two possible interpretations that take into account the equivalence question within the conductive layer. Both are of an equal quality when looking to the fit, and the solutions only differs within the conductive layer, that is one has a  $2.1 \Omega \cdot m$  with a 6.4 m thickness in the first interpretation, and a  $11.4 \Omega \cdot m$  with a 13.2m thickness in the second interpretation. However, in the first case the recomputed EM31 conductivity is about 40 mS/m, while in the second case is 26 mS/m, which is much closer to value found on the EM31 map at this point (about 20 mS/m). Hence the second interpretation is more realistic.

This is of great importance here. Indeed, a  $2.1 \Omega \cdot m$  layer would be a salted layer, while  $11.4 \Omega \cdot m$  is probably just a clayey and very wet (saturated) zone (of course we cannot exclude the presence of some salt). Moreover the interpretation of thicknesses also depends on the relevancy of the interpretation.

To conclude: SEV02 and SEV06 are both in resistive patches of the EM31. The first shows a mean resistivity at depth and could correspond to a vadose zone with some residual capillary water. The shallow conductive layer is probably due to a more clayey horizon. The second is definitely resistant until a depth of about 5 meters. Since a conductive layer is then reached, one can suppose that this area is very permeable. This will both explain the two facts: i) the vadose zone is drained and hence resistive, and ii) a water sheet is possible at the bottom of this layer just above less permeable bedrock<sup>19</sup>.

From the confrontation with the EM31, we can state a rule: as conductive layer are concerned, and within an equivalence set, the less conductive and thicker layer seems to be the best choice.

Why one cannot does fully join the two approaches, that is why does the conductivity of the EM31 seem lower than the one derived from the electrical sounding? In my opinion, it is due to the fact

<sup>19</sup> Of course, geophysics alone is extremely speculative, and the geophysicists cannot be very affirmative before some drilling check what is only hypothesis at this stage.

that the Slingram is inductive and hence more sensitive to *conductive* media. As an example if we imagine some confined conductive bodies in the ground, EM31 will see them much better than galvanic methods.

3) SEV05 and SEV03 are made on conductive patches.

SEV05 is very robust, with a first resistive layer at  $305 \Omega \cdot \text{m}$  and a thickness of 30 cm, then a 11.6 m thick layer at  $30 \Omega \cdot \text{m}$  and below that  $90 \Omega \cdot \text{m}$  bedrock.

I argue that the first resistive layer will correspond to the 0+A horizons, and that B and C cannot easily be distinguished on that sounding (at least during the dry season) by their electrical properties.

However, this must be confirmed by soil scientists.

The SEV03 sounding allows several equivalent interpretations. Let us see if it confirms our new rule. The first layer is close to  $440 \Omega \cdot \text{m}$  with 19 cm of thickness. The second layer is at  $30 \Omega \cdot \text{m}$ . In the first interpretation, it is 3.24 m thick, and below there is a very conductive layer at  $1.78 \Omega \cdot \text{m}$  with an only 0.4 m thickness. In the second interpretation, the  $30 \Omega \cdot \text{m}$  layer has a thickness of 2.35 m (1 meter less than the previous hypothesis) and the conductive layer is at  $16 \Omega \cdot \text{m}$  with a 4.3 thickness. Both hypotheses finish with a  $78 \Omega \cdot \text{m}$  lower medium.

The resistivity as seen on the EM31 map is 34 mS/m.

Computing the conductivity in the first hypothesis leads to a value of 40 mS/m while in the second case it is 34 mS/m, excellent agreement. We can adopt the rule to deal with equivalences: it seems better to take the most resistant extreme of the equivalence domain.

Now we have here two conductive layers, the first ( $30 \Omega \cdot \text{m}$ ) stops at about 2.5 depths, and the following is more conductive ( $16 \Omega \cdot \text{m}$ ) before reaching the resistive bedrock. Could this thickness correspond to the horizon B, where roots are drying the soil?

4) SEV4. It is in a special area, close to the gully and near a big acacia. Its end (the deeper investigation) brushes again the gully and this could raise the resistivity, but the beginning of the sounding is robust with respect to that event.

This VES is of interest for an additional reason: this area is expected to be well-drained by the big ditch nearby. Here we have a 0.33 m of resistant soil, then almost two meters at  $54 \Omega \cdot \text{m}$  and then a  $35 \Omega \cdot \text{m}$  with a 12.5 m thickness. The last layer is above  $80 \Omega \cdot \text{m}$ . It resembles SEV03.

5) Let now consider the two northern VES SEV07 and SEV08.

SEV07 is unique in our set, since it is the only sounding where the resistivity remains over  $100 \Omega \cdot \text{m}$ . No doubt that the geology is quite different in this resistive area.

SEV08 is completely different. First we have the usual resistive layer between 180 and  $400 \Omega \cdot \text{m}$  at the surface. But the conductive layer at  $20 \Omega \cdot \text{m}$  is reached at a depth of 40 or 50 cm, and then shows a 10 m thickness. Deeper it becomes resistant again with a resistivity of  $165 \Omega \cdot \text{m}$ .

One more time one can consider that this conductive medium is drained due to the vicinity of the gully. However, this area is more humid than the catena, since it is much less steep. Moreover, it is possible that the resistive part at the North forms a sort of dam which prevents water to run down or at least slow it down it. However the season lead us to suppose that the subsurface is not saturated here.

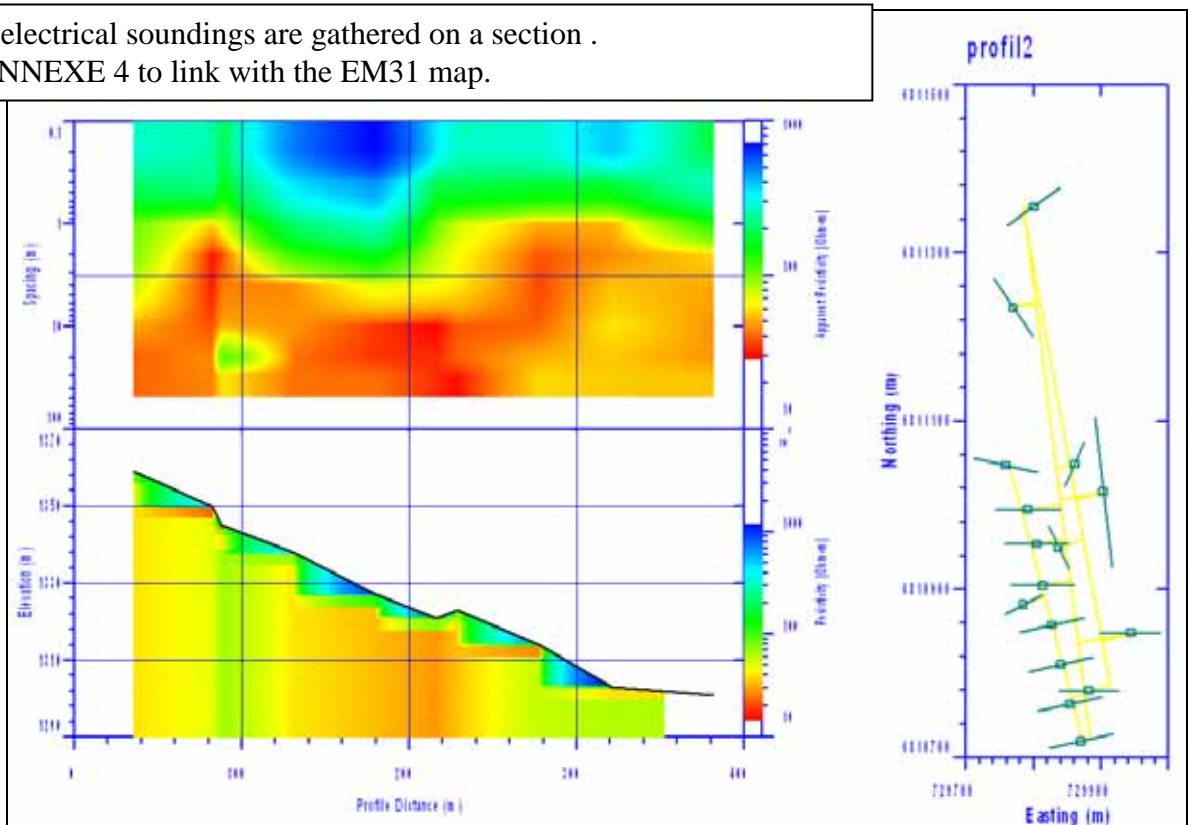
- 6) We deal now with the toposequence that is soundings made with a regular step of 50 m, along the steepest descent, where other data are usually collected.

Actually the regular step was not a fully good idea, since some of the soundings are at the boundary between conductive and resistive layers. Nevertheless, let's gather the most relevant facts:

- in all cases, we have first a resistant soil layer (more than  $100 \Omega \cdot m$ ). Its thickness is variable: In some cases it is followed directly by a conductive layer (ts02, ts06, ts07) or an additional but less resistant layer may exist till 1 m (typically ts01, ts03, ts04, maybe ts05);
- a conductive layer does exist, between 20 and  $40 \Omega \cdot m$ , everywhere. Since this resistivity is lower than the water itself (which is close to  $70 \Omega \cdot m$ ), this layer clearly contains clay, but not a great amount so it is permeable;
- none of these soundings allows us to determine with reliability the resistivity of the deepest observed layer. However all are compatible with the bedrock resistivity as seen by the deeper sounding (sev03), which is  $80 \Omega \cdot m$ . Time domain sounding should provide additional information at these depths.

The electrical soundings can be gathered on various representation modes. For instance, here is one relative to the toposequensis of Figure 21:

Figure 21: electrical soundings are gathered on a section .  
See also ANNEXE 4 to link with the EM31 map.



This Figure shows: at right the plane geometry, with sounding locations and relative profile. The toposequensis is the straight line at the left lower part of the figure (equally spaced VES).

Top left is the pseudo-section interpolated from the VES (that is, a 2-D colour representation of the apparent resistivities) and bottom left is an inverted resistivity structure which is compatible with the data. Although this plot is obtained from a professional code, I don't like the effects it can produce in the interpreter. Such a resistivity stair is appealing... but does not exist.

### 3. Electrical resistivity tomography (ERT).

The method became very popular since the availability of easy-to-use codes to invert data and efficient multi-electrode commutating systems. The most used code is from Loke (all resources are at <http://www.geoelectrical.com/>, including an important bibliography);

Basically, the ERT is nothing but an electrical array in which we make by varying both location and depth investigation along a profile. We plot a section in the data space (with location and depth), but since it concerns apparent resistivity it is not indicative of real depths. Hence this section is named "pseudo-section", and it is *only* a data representation mean in which the "pseudo-depths" are not relevant. A sophisticated least-square method is used to invert the data (all info on the site above!), and then produces a real section, with true resistivities, but with a poor resolution<sup>20</sup>.

With modern apparatus, the geophysicist dispatches a set of electrodes along a profile. A multiplexor switches the system and the apparatus collects the data in the internal memory.

In Potshini, geophysicists made use of the Terrameter from ABEM. Some adaptations were required and are related in ANNEXE 3 (thanks to Myriam).

The section is located along the toposequense. The inter-electrode spacing is 2 m and the profile is almost 400 m long. Some 2 m data are missing in the second part of the profile.

With this spacing, resistivity cannot be inverted in the first 50 cm, so this first ERT in Potshini is devoted to the mean depths, saying 1 to 10 m.

The results are shown on Figure 22. The geometrical-geoelectrical patterns become clear. At a mean depth, one can see a succession of conductive ( $10 \Omega \cdot \text{m}$ ) and more resistive ( $100 \Omega \cdot \text{m}$ ) regions which could correspond to the beddings with alternating low and high clay content.

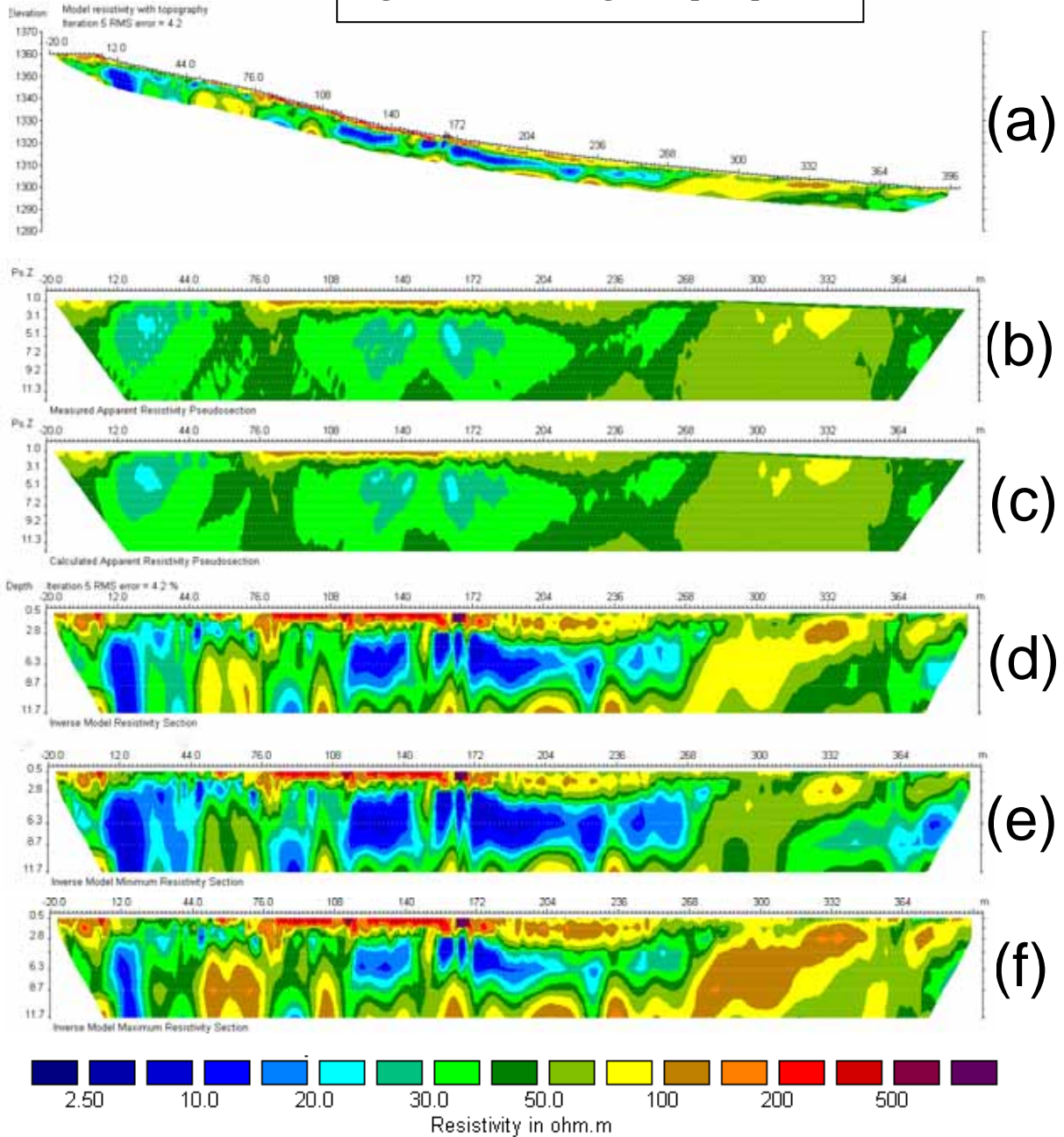
Close to the surface, we can see where the slope is the steeper that the ground is resistive until a 2 m depth. Waters may have completely run-off from this area.

Further fieldwork with mechanical soundings will undoubtedly light up these results, and we look for the data during the wet season.

---

<sup>20</sup> The resolving power of a method is directly linked with the Green's function of the physical law. In electricity, it is  $1/r$ . One can consider that the resolution at a given depth is more or less the third of the depth.

Figure 22: ERT along the toposequensis



- (a) inverted section with topography
- (b) effective data
- (c) theoretical data computed from inverted model
- (d) like (a) but without topo and with vertical exgeration
- (e) minimum model
- (f) maximum model

*N.B. The little bevel at the right edge of (b) and (c) is due to the missing of some data in that part (lack of time).*

#### 4. Time Domain Electro-Magnetic soundings (TDEM)

The device is the “Temfast 48 HPC”.

Numerous examples of applications and related papers can be found at <http://www.aemr.net/>.

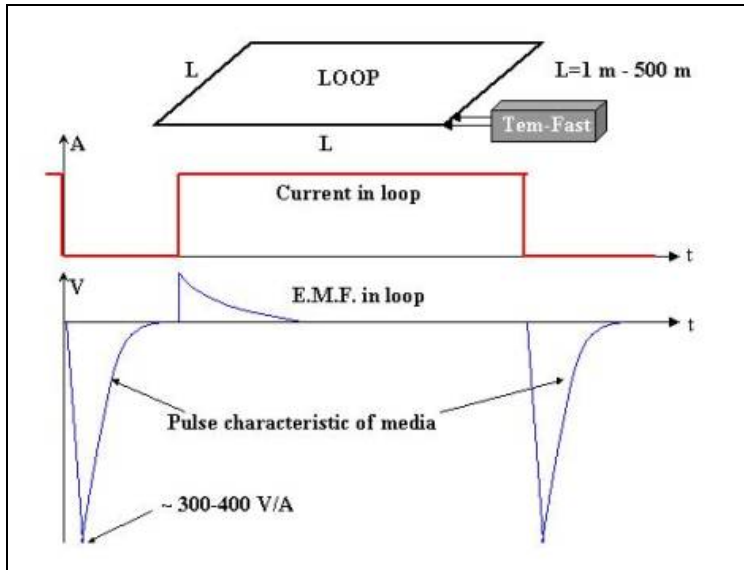


Figure 23: TDEM sounding principle

The TDEM sounding method is based on the following. A horizontal current wire loop emits an EM impulse in the space. It produces “eddy” currents in the ground, which spread deeper and deeper and also decay in amplitude and wider. Those currents produces a secondary magnetic field which is detected in a secondary coil or in the transmitter itself.

See Figure 23 and 24.

Actually the method is based on the same asymptotic figure of Maxwell’s equation set than for the EM31 (that is, the inductive limit), but the application is quite different and involves transient signals instead of pure sinusoidal ones.

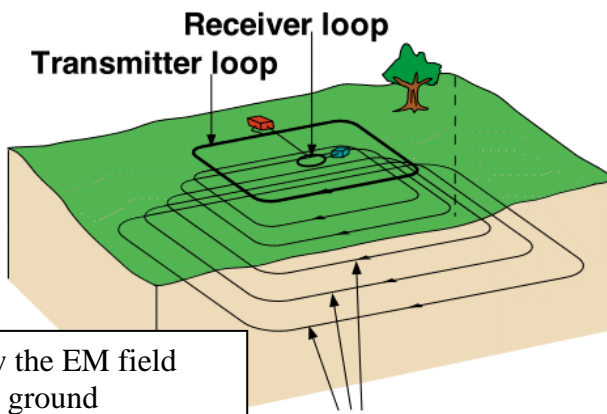


Figure 24: how the EM field spread into the ground

**induced eddy currents at progressively later times after turnoff**

The measured parameter is the secondary magnetic field (the primary has been shut down), and the longer the listening, the deeper the recovered signal. In the case of a homogeneous medium, the field follows the law given in BOX 9. From that one derives an apparent resistivity (versus time) which can be

inverted into resistivity versus depth.

inverted into resistivity versus depth.

### BOX 9: TDEM sounding

If we use one circular loop of radius (a) and a current I over a homogeneous half space of resistivity  $\rho$ , the secondary magnetic field time variation as it can be measured in the same loop is given by:

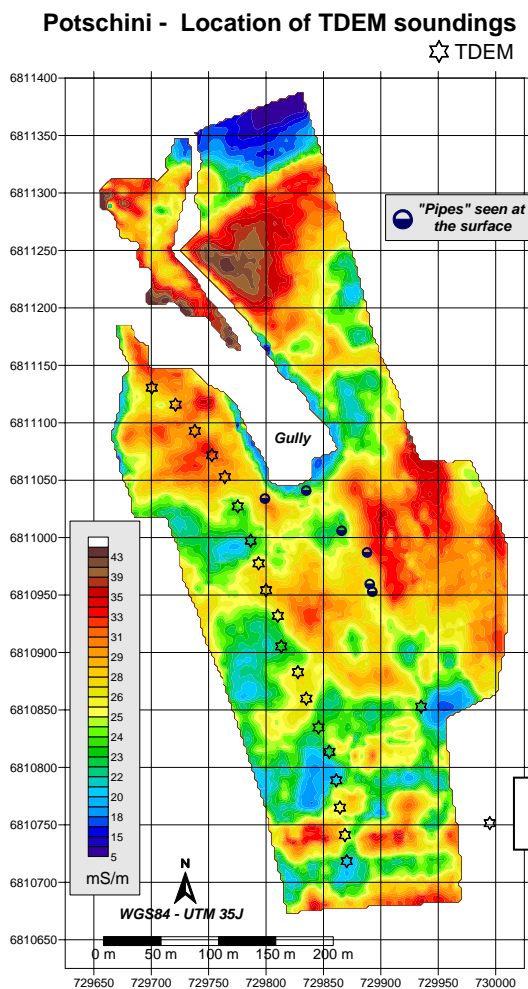
$$\frac{\partial B_z}{\partial t} \cong -\frac{I \rho^{-\frac{3}{2}} \mu_0^{\frac{5}{2}} a^2}{20\sqrt{\pi}} t^{-\frac{5}{2}}.$$

It decays like  $t^{-\frac{5}{2}}$ , and this is linear on a log scale. The apparent resistivity is obtained by inverting this formula as a function of time (t), that is:

$$\rho_a = \left( \frac{I^2 a^4 \mu_0^5 t^{-5}}{400\pi (\partial B_z / \partial t)^2} \right)^{\frac{1}{3}}.$$

The apparent resistivity curve also follows the resistivity ground conformation, but it can show additional oscillations and then the inverse code is definitely required to derive the structure.

The Figure 25 shows the location of the TDEM soundings.



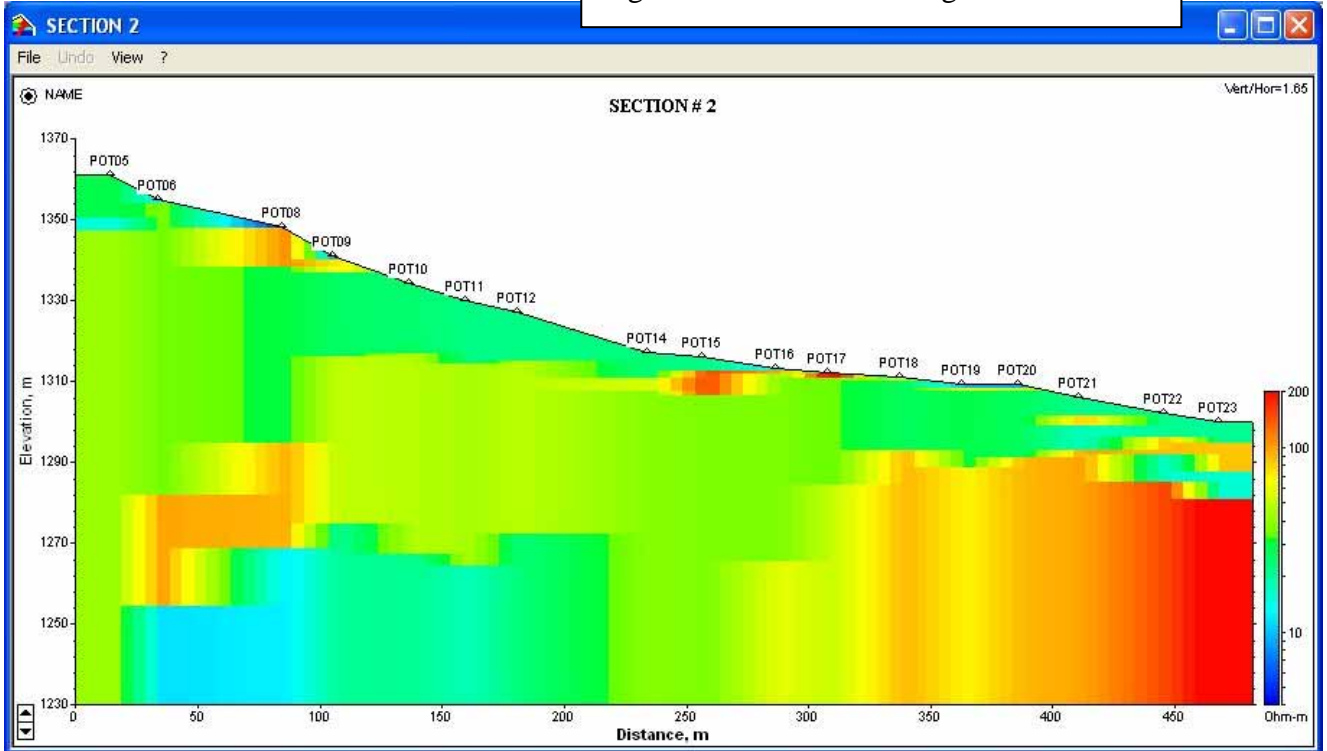
Since the density of soundings is relatively high, the reliability in gathering them into a unique section is fair. A few soundings have been removed due to the coupling with some sheep wires. It finally provides the figure below.

There are two features that contrast with the VES method: i) the TDEM sees deeper, and 2) is more sensitive to conductive layers. One observes on the figure that the mean resistivity is, in green or yellow-green, close to 20 to 40, as expected from VES and EM31. In depth, a great difference occurs between the north which is resistive, and the south which seems more conductive. On the north part, at the right on the figure, a resistive body is encountered at a depth of 20 meters, and the conductive layer above could be some water accumulation flowing on that less permeable bedrock.

Figure 25 : location of TDEM soundings

Finally one can plot also a section that gathers the soundings on a unique image, Figure 25.

Figure 26: TDEM sounding as a section



Close to the top (1350 m) and in the middle (1310m), the shallow resistant body may be consolidating sandstone banks outcropping. But one of the main features could be here the resistant structure at the bottom right of the section, where the contrast with the other part is significant. The orange to red colourings are relative to very resistant rocks (100 to 200  $\Omega$ .m) with respect to the blue to green parts which correspond to clayey or/and wet rocks between 10 and possibly 50  $\Omega$ .m .

## CONCLUSION

This first report shows the potential of geophysical methods to investigate Potshini catchment. In particular, the EM38 strategy is expected useful to characterize the A soil horizon. This must be investigated deeper, both in terms of cognition and in terms of physical soundings!

In this report, we did not go deeply into exploring our data set. For instance, a more systematic comparison between the various methods is still to be done.

Nicolas Florsch and the whole Potshini team  
November 2008

## References

- Archie, G.E., 1942. The electrical resistivity log as an aid in determining some reservoir characteristics, *Trans. Amer. Inst. Mining Metallurgical and Petroleum Engineers*, 146, 54-62.
- Binley, A., L. D. Slater, M. Fukes, and G. Cassiani (2005), Relationship between Spectral Induced Polarization and hydraulic properties of saturated and unsaturated sandstone, 318, *Water Resour. Res.*, 41, 12, W12417, doi: 10.1029/2005WR004202.
- Florsch N. and Hinderer J. 2000. Bayesian estimation of the free core nutation parameters from the analysis of precise tidal gravity data. *Physics of the Earth and Planetary Interiors* 117, 21–35.
- Ghorbani, A., Camerlynck, C., Florsch, N., Cosenza, P., and Revil, A., 2007. Bayesian inference of the Cole–Cole parameters from time- and frequency-domain induced polarization. *Geophysical Prospecting*, 2007, 55, 589–605
- Giroux, B. and Chouteau, M. 2008. A hydrogeophysical synthetic model generator, *Computers & Geosciences*, Volume 34, Issue 9, Pages 1080-1092.
- Keller, G., 1987. Rock and mineral properties, in *Electromagnetic Method in Applied Geophysics- Theory, V.1, M.N. Nabighian, ed, Society of Exploration Geophysicists, Tulsa, Oklahoma.*
- Kemma, A, Binley, A., Ramirez, A.L., and Daily W.D., 2000. Complex resistivity tomography for environmental applications, *Chem. Eng. J.*, 11-18.
- Menke, W., 1989. *Geophysical data analysis: Discrete inverse theory*, Academic Press, San Diego.
- Pride, S., 1994. Governing equations for the coupled electromagnetics and acoustics of porous media, *Phys. Rev. B* 50, 15678 - 15696 (1994)
- Rhoades, J.D., Ratts, P.A.C. and Prather, R.J., 1976. Effects of liquid-phase electrical conductivity, water content and surface conductivity on bulk soil electrical conductivity, *Soil Sci. Soc. Am. J.*, 40, 651-655.
- Schön, J.H., 1996. Physical properties of rocks – fundamentals and principles of petrophysics. Elsevier Science Ltd., *Handbook of Geophysical Exploration*, 18, 379-479.
- Tarantola A. and Valette B. 1982. Inverse problems - Quest for in-formation. *Journal of Geophysics* 50, 159–170.
- Tarantola A. 1987. *Inverse Problem Theory, Methods for Data Fitting and Model Parameter Estimation.* Elsevier Science Publishing Co.
- Tarantola A. 2004. *Inverse Problem Theory and Model Parameter Estimation.* SIAM.
- Waxman, M.H., and Smits, L.J.M., 1968. Electrical conductivities in oil-bearing shaly sands, *Soc. Pet. Eng. J.*, 8, 107-122.

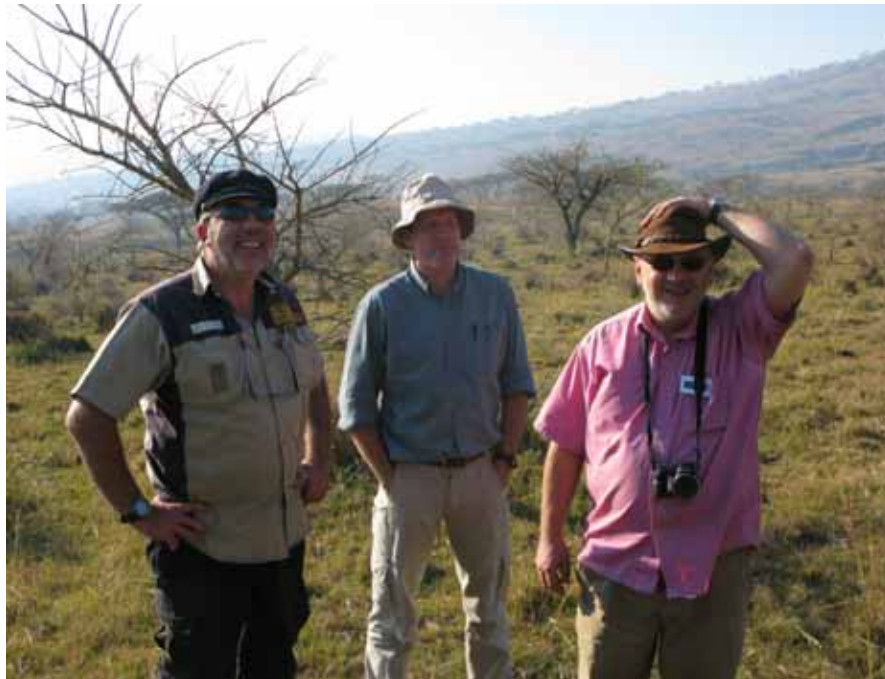
## ANNEXE 1: perspectives and examples of things to do...

In completing this report:

- Georeference B71 EM38 map
- Drape all geophysical data sets on topography
- Redo EM31, EM38, and ERT to get time-lapse data, possibly at two opposed seasons since the actual data have to been acquired in the best condition (as a beginning)
- Map SP at the most run-off period (just wait the rain stops because it makes the SP signal noisy)
- In general correlate the different methods to light up the structures and improve the geometrical model
- At least, create an hydrological and soil geometrical model based on these data

Making science

- Study the interactions between soil features as seen by geophysics and plants...
- Use geophysical data into hydro-ecological model
- Improve EM38 use for topsoil characterization
- Write papers on these points



## ANNEXE 2

Water conductivities (thanks to Jean-Louis)

Sample number	Sample area	(rough) Altitude (Meter)	Lat- lon	UTM	Cond (Microsiemens/)	Temp (Celsius)	Date
1	Thalweg of Gully (3 sites -distance 10m) Water Surface	1251	S28 48 20.4 E029 21 12.9	35J 0729703 6811260	149	26	23/09/2008
					137	27,7	
					142	26,1	
2	Gully down stream (3 sites -distance 10m) Water Surface	1254	S28 48 18 E02921 13.7	35J029723 6811344	167	27,6	23/09/2008
					167	26,6	
					167	26,4	
3	Gully (Middle slope) (3 sites -distance 10m) Water Surface	1256	S28 48 22.8 E029 21 10.9	35J0729646 6811197	138	24,6	23/09/2008
					138	24	
					137	25,2	
4	Gully (Middle slope) (3 sites -distance 10m) 5cm Water depth to surface	1266	S28 48 23.3 E029 21 10.7		143	17	23/09/2008
					140	21,6	
					141	23,4	
5	Gully - Up-stream (3 sites -distance 10m) Water Surface	1272	S28 48 26.6 E029 21 09.6	35J0729615 6811081	139	27,8	23/09/2008
					139	28,6	
					140	27,6	
6	Gully up-stream (the highest) (3 sites -distance 10m) Water Surface	1278	S28 48 29.1 E029 21 094	35J0729600 6811005	134	24,5	23/09/2008
					134	24,7	
					135	24,8	
7	Water well	1324	S28 48 41.8 E029 21 54.2		241	20,5	23/09/2008
					241	19,3	
					241	19,2	

The measurement are done 48h after a rain of 30mm first runoff of the rainy season



## ANNEXE 3 (written by Myriam)

### How to use Pietermaritzburg ABEM Terrameter 1000 (PMB) ?

#### 1. Equipment

Take care, 64 connections on the resistivimeter on one side, whereas 4 cables of 21 connections (84) on the other side: that makes almost all difficulties and is very time consuming for roll along

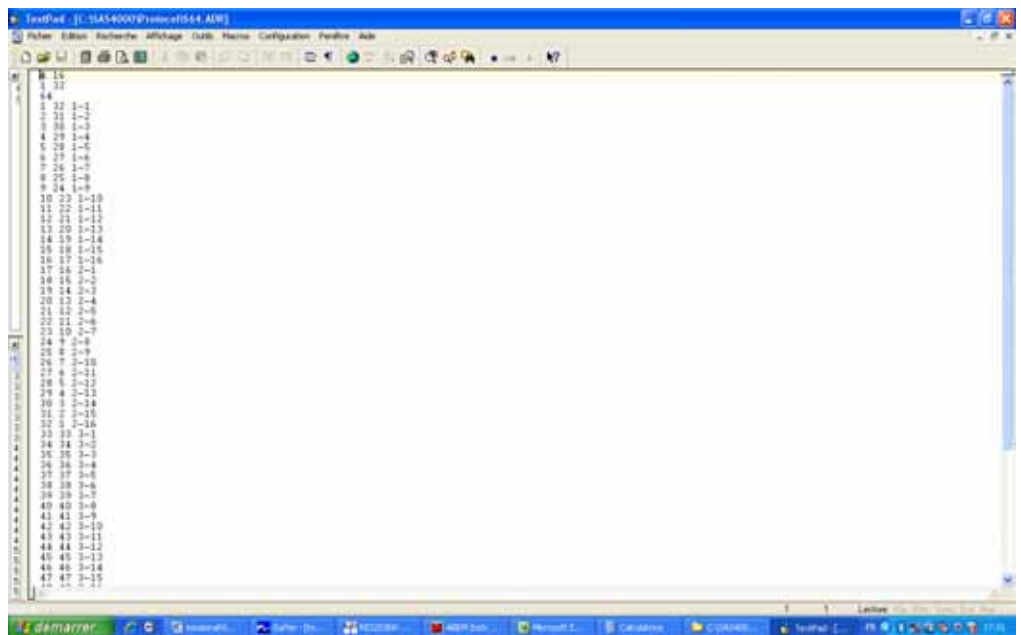
#### 2. Files to be prepared

Sequences (.org) : the sequences might be prepared for 64 electrodes, but Geonics proposes 61. I did not have time enough to check why.

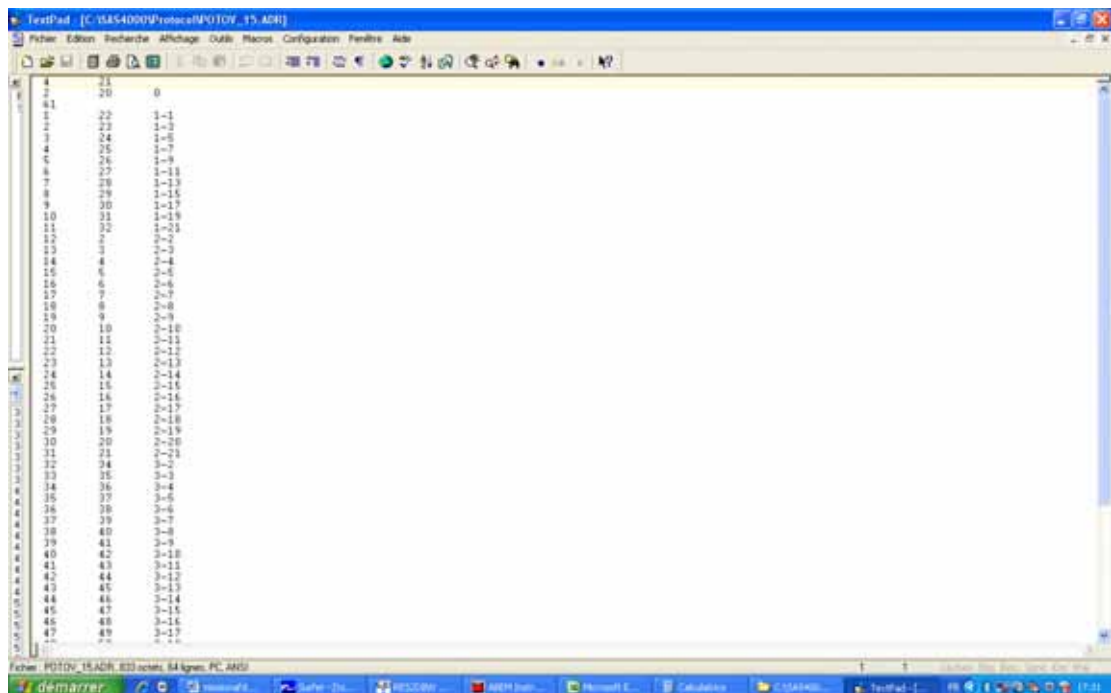
Address files (.ADR) : totally different from newest version of Terrameter 1000

Exemple to do the same

On newest version:

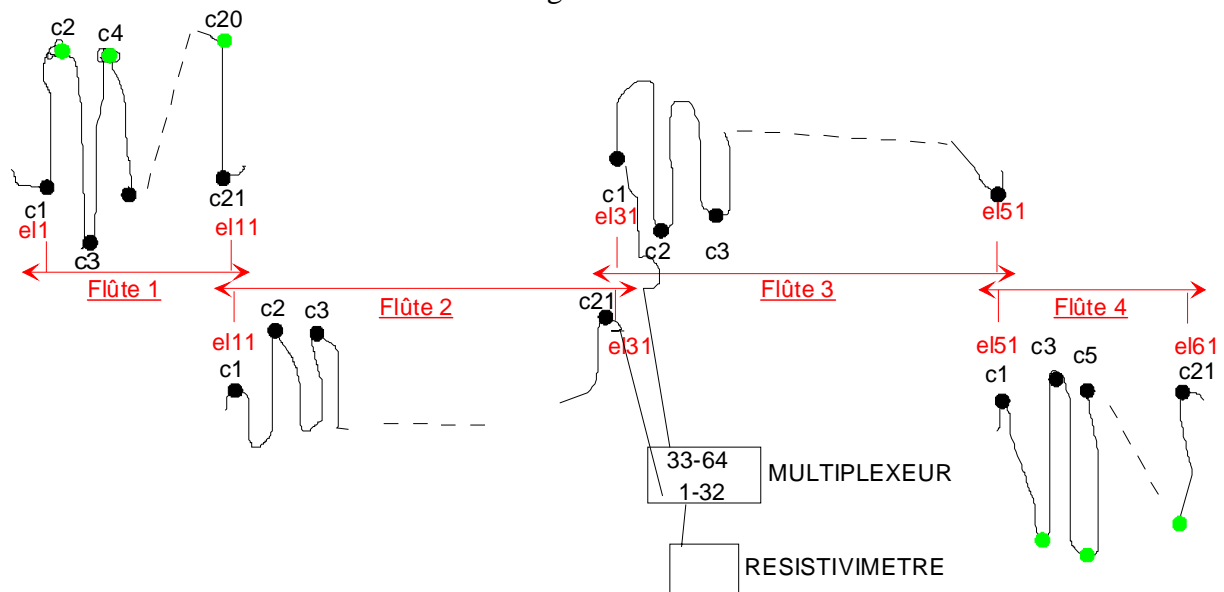


On PMB version:



### 3. On the field

Cables have to be connected like this using 61 electrodes.



● connections des flûtes reliées aux électrodes

● connections des flûtes non reliées aux flûtes

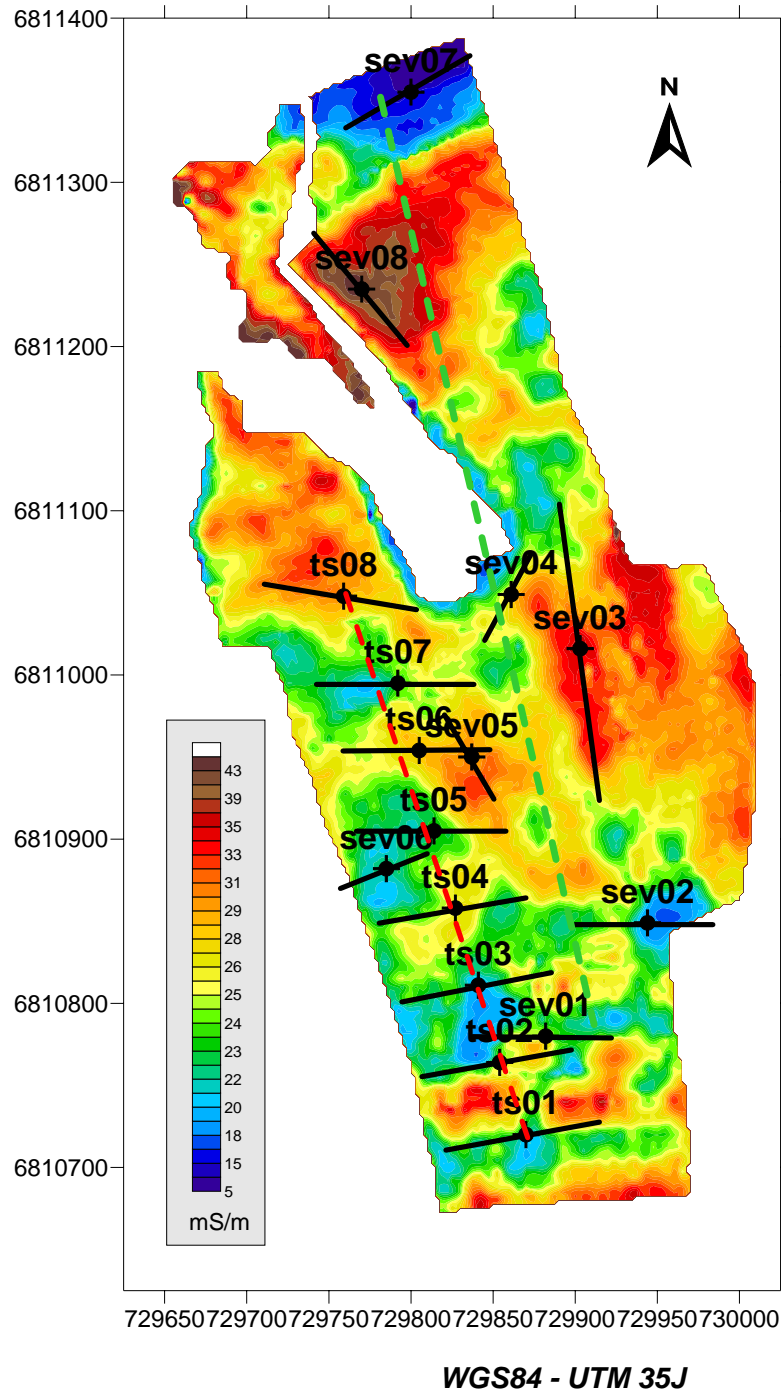
Remark for roll along :

If you would have the same number of connections on the cables (instead of 84, only 64) and on the resistivimeter (64), you would decrease the installation period of about 30%, because the device would be equivalent. Otherwise (in your case), the device is symmetrical around the device center. Thus at each shift, you have to disconnect everything, and thus reconnect everything in a different way.



ANNEXE 4: location of VES

Potschini - Location of VES on the EM31 map



That's all folks